Cusped SYM Wilson loop at two loops and beyond

Yuri Makeenko*

Institute of Theoretical and Experimental Physics

117218 Moscow, Russia

Poul Olesen*

The Niels Bohr Institute

Blegdamsvej 17, 2100 Copenhagen Ø, Denmark

Gordon W. Semenoff

Department of Physics and Astronomy, University of British Columbia

Vancouver, British Columbia, Canada V6T 1Z1

Abstract

We calculate the anomalous dimension of the cusped Wilson loop in $\mathcal{N} = 4$ supersymmetric Yang-Mills theory to order λ^2 ($\lambda = g^2_{YM}N$). We show that the cancellation between the diagrams with the three-point vertex and the self-energy insertion to the propagator which occurs for smooth Wilson loops is not complete for cusped loops, so that an anomaly term remains. This term contributes to the cusp anomalous dimension. The result agrees with the anomalous dimensions of twist-two conformal operators with large spin. We verify the loop equation for cusped loops to order λ^2, reproducing the cusp anomalous dimension this way. We also examine the issue of summing ladder diagrams to all orders. We find an exact solution of the Bethe-Salpeter equation, summing light-cone ladder diagrams, and show that for certain values of parameters it reduces to a Bessel function. We find that the ladder diagrams cannot reproduce for large λ the $\sqrt{\lambda}$-behavior of the cusp anomalous dimension expected from the AdS/CFT correspondence.

*Also at the Institute for Advanced Cycling, Blegdamsvej 19, 2100 Copenhagen Ø, Denmark

1 Introduction

The cusped Wilson loop has a number of applications to physical processes. It represents the world trajectory of a heavy quark in QCD which changes its velocity suddenly at the location of the cusp. For Euclidean kinematics, or when it is away from the light-cone in Minkowski space, the cusped Wilson loop is multiplicatively renormalizable (for a review see Ref. [1] and references therein). In that case, the ultraviolet divergence is associated with the bremsstrahlung radiation of soft gluons emitted by the quark during its sudden change in velocity. The cusp anomalous dimension $\gamma_{\rm cusp}$ depends on θ, the variable which represents, as is depicted in Fig. 1, either the angle at the cusp in Euclidean space or the change of the rapidity variable in Minkowski space.

At large θ the cusp anomalous dimension is proportional to θ:

$$\gamma_{\rm cusp} = \frac{\theta}{2} f(g_{YM}^2, N)\,. \tag{1.1}$$

The function $f(g_{YM}^2, N)$ can be calculated perturbatively. In the planar limit, which we shall discuss exclusively in the following, it is a function of the 't Hooft coupling $\lambda = g_{YM}^2 N$. It is related [2, 3, 4, 5] to the anomalous dimensions of twist-two conformal operators [6] with large spin J in QCD by

$$\gamma_J = f(\lambda) \ln J\,. \tag{1.2}$$

In the limit of large θ, the segment of the Wilson loop approaches the light-cone where the contribution of higher twist operators are suppressed.

Interest in the anomalous dimensions of the twist-two operators was inspired by Gubser, Klebanov and Polyakov [7] who calculated the leading Regge trajectory of a closed string in type IIB superstring theory propagating on the background space-time $AdS_5 \times S^5$. They considered the string rotating on AdS with large angular momentum. According to the AdS/CFT correspondence [8, 9, 10] (for a review see Ref. [11]) this trajectory is related to the γ_J in $\mathcal{N} = 4$ supersymmetric Yang-Mills theory (SYM) and predicts[3]

$$f(\lambda) = \frac{\sqrt{\lambda}}{\pi} + \mathcal{O}\left((\sqrt{\lambda})^0\right) \tag{1.3}$$

for large λ. This result is obtained for large spin J, which plays the role of a semiclassical limit in analogy with the BMN limit [13], and there was argued in Ref. [7] that it possesses the features expected for the anomalous dimension in QCD and may remain to be valid there as well.

Alternatively, the cusp anomalous dimension in $\mathcal{N} = 4$ SYM can be directly calculated using the duality [14, 15, 16, 17] of the supersymmetric Wilson loop and an open string in $AdS_5 \times S^5$, the ends of which run along the contour $\{x^\mu(s), \int^s {\rm d}s' |\dot{x}(s')| n^i\}$ (where $n^i \in S^5$) at the boundary of $AdS_5 \times S^5$.

[3]The $(\sqrt{\lambda})^0$-contribution to this formula, $-3 \ln 2/\pi$, was calculated in Ref. [12].

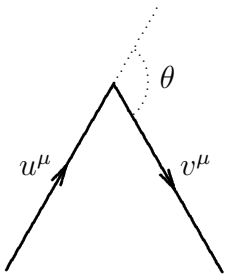

Figure 1: Cusped Wilson loop analytically given by Eq. (2.1).

The relevant Wilson loop [14]

$$W(C) = \frac{1}{N}\mathrm{Tr}\,\boldsymbol{P}\, e^{i\int_C ds\dot{x}^\mu(s)A_\mu(x)+i\int_C ds|\dot{x}(s)|n^i\Phi_i(x)} \tag{1.4}$$

contains the scalar fields $\Phi_i(x)$ of $\mathcal{N}=4$ SYM as well as the gauge field. This expression applies to Minkowski space. In Euclidean space, the factor of i is absent from the scalar term. When $\dot{x}^\mu$ is null, $|\dot{x}|=0$, as happens when the contour occupies the light-cone in Minkowski space, the scalar contribution vanishes and this operator coincides with the usual definition of Wilson loop in gauge theory.

In the supergravity limit, the string worldsheet coincides with the minimal surface in $AdS_5\times S^5$ bounded by the loop. Computing the proper area of this surface determines the asymptotic behavior of the Wilson loop for large λ. This approach was first applied to the cusped Wilson loop, depicted in Fig. 1, in Ref. [17]. It was used in Refs. [18, 19] to reproduce the strong-coupling result (1.3).

There are a number of circumstances where the strong coupling asymptotics of Wilson loops can be obtained by summing planar ladder diagrams. For the case of anti-parallel Wilson lines, for example, the sum of planar ladders [20] produces the $\sqrt{\lambda}$ behavior that is found using AdS/CFT [14, 15], but fails to get the correct coefficient of the quark-antiquark potential. For the circular Wilson loop, the sum of planar ladder diagrams can be done explicitly and extrapolated to the strong coupling limit [21] where it is in precise agreement with the prediction of AdS/CFT. In that case, it has been argued that the sum of planar ladders obtains the exact result for the Wilson loop in the 't Hooft limit. A similar argument can be made for the correlation functions of chiral primary operators with the circular Wilson loop which are also thought to be given exactly by the sum of planar ladder diagrams which can be performed explicitly and agrees with AdS/CFT [22]. In addition to providing a test of AdS/CFT duality, these results make a number of challenging predictions for IIB superstrings on the $AdS_5\times S^5$ background [23, 22] (for a review see Ref. [24]).

A natural question is whether the strong coupling asymptotics (1.3) for the cusped loop can be obtained from supersymmetric Yang-Mills perturbation theory. To examine this, we shall begin at weak coupling by computing the leading perturbative contributions to the cusped loop to order λ^2. In this computation, we observe that the divergences which

lead to the anomalous dimension of the loop arise from two sources, ladder diagrams and an incomplete cancellation of divergent diagrams with internal vertices. The latter is in contrast to smooth loops where, to order λ^2, the divergent parts of diagrams with internal vertices cancel. In fact, for loops with special geometry, such as the circle or straight line, their entire contribution cancels. It is this cancellation which leads to the mild ultraviolet properties of the SYM Wilson loop (1.4) which were discussed in Ref. [17]. In the case of the cusped loop, this lack of cancellation already implies that the cusp anomalous dimension cannot come from ladder diagrams alone, it must obtain contributions both from diagrams with internal loops and from diagrams with ladders.

The result for the anomalous dimension of the cusped SYM Wilson loop to the order λ^2 agrees with the two-loop anomalous dimension [25, 26, 27, 28, 29] of twist-two conformal operators with large spin J in $\mathcal{N} = 4$ SYM, calculated using regularization via dimensional reduction:

$$f(\lambda) = \frac{\lambda}{2\pi^2} - \frac{\lambda^2}{96\pi^2} + \frac{11\lambda^3}{23040\pi^2} + \mathcal{O}\left(\lambda^4\right). \tag{1.5}$$

Here the three-loop term $\sim \lambda^3$ was obtained in the recent calculation of Ref. [30] and reproduced [31] from the spin-chain Bethe ansatz. Equation (1.5) also agrees with the two-loop calculation [3, 32] of the cusp anomalous dimension of the non-supersymmetric Wilson loop.

The question that remains asks whether the sum of ladder diagrams can produce a contribution to the cusp anomalous dimension which resembles (1.3) at strong coupling. In fact, this was suggested as the source of the $\sqrt{\lambda}$ strong coupling behavior in Section 5 of Ref. [7] in the context of large spin. The situation for the cusp could be similar and closely analogous to that in Ref. [20] for the sum of the ladder diagrams in the case of antiparallel Wilson lines, there the sum of ladders exhibits the $\sqrt{\lambda}$-behavior at large λ but it is suspected that other diagrams also contribute, and must be included if the full answer is to match the prediction of AdS/CFT.

In this Paper, we shall examine the issue of summing (rainbow) ladder diagrams contributing to the cusped loops to all orders. We shall find an exact solution of the Bethe-Salpeter equation, which sums light-cone ladder diagrams. We shall show that for certain values of parameters it reduces to a Bessel function.

We shall also observe that its asymptotic form indeed contains a $\sqrt{\lambda}$ term, but it does not contain the leading term in the rapidity angle θ in (1.1). This means that ladders are not the answer at strong coupling, beyond the first few orders their sum is sub-leading at large θ. A similar situation has been observed for the wavy Wilson line [33]. There, to leading order in the waviness, AdS/CFT predicts that the line has a $\sqrt{\lambda}$ dependence. In that case, by examining Feynman diagrams, one concludes that the contributions are given entirely by non-ladder diagrams. In the present case, we could speculate that the diagrams which contribute are more likely of the form of the ones having legs frozen at the location of the cusp, perhaps with several lines from internal vertices trapped at the cusp.

In addition, a particular form of the loop equation in $\mathcal{N}=4$ SYM was formulated in Ref. [17]. There, it was observed that for the cusped loop the right-hand side of the loop equation is proportional to the cusp anomalous dimension calculated to one loop order in $\mathcal{N}=4$ SYM perturbation theory. In this Paper, we will re-examine this issue with an explicit computation to order λ^2 that confirms that for the cusped loop the loop equation reproduces the cusp anomalous dimension to order two loops in SYM perturbation theory.

This Paper is organized as follows. In Sect. 2 we analyze the two-loop diagrams with internal vertices and show that the cancellation is not complete in the presence of a cusp. This results in an appearance of the anomalous boundary term. In Sect. 3 we calculate the cusp anomalous dimension for Minkowski angles θ and find its asymptotic behavior for large θ. The result agrees with the anomalous dimension of twist-two conformal operators with large spin. In Sect. 4 we verify the loop equation for cusped loops to order λ^2, reproducing the cusp anomalous dimension this way. In Sect. 5 we find an exact solution of the Bethe-Salpeter equation, summing light-cone ladder diagrams, and show that for certain values of parameters it reduces to a Bessel function. A conclusion is that the ladder diagrams cannot reproduce for large λ the $\sqrt{\lambda}$-behavior of the cusp anomalous dimension expected from the AdS/CFT correspondence. The results and further perspectives are discussed in Sect. 6.

2 Graphs with internal vertices

2.1 Kinematics

Let us parametrize the loop by a function $x_\mu(\tau)$. The cusped Wilson loop depicted in Fig. 1 is then formed by two rays:

$$x_\mu(\tau) = \begin{cases} u_\mu \tau & (\tau < 0) \\ v_\mu \tau & (\tau \geq 0)\,, \end{cases} \tag{2.1}$$

while the cusp is at $\tau = 0$. The cusp angle is obviously given by

$$\begin{aligned} \cos\theta &= \frac{uv}{\sqrt{u^2}\sqrt{v^2}} \qquad \text{Euclidean space}\,, \\ \cosh\theta &= \frac{uv}{\sqrt{u^2}\sqrt{v^2}} \qquad \text{Minkowski space}\,. \end{aligned} \tag{2.2}$$

The nontrivial two-loop diagrams that contribute to the cusped Wilson loop in Fig. 1 are depicted in Fig. 2. The diagram in Fig. 2(l) is of the type of a ladder with two rungs. The diagrams in Figs. 2(b) and (c) involve the interaction given by the three-point vertex, while the diagram in Fig. 2(d) is of the type of a self-energy insertion to the propagator.

2.2 The anomalous surface term

The analysis of the diagrams in Figs. 2(b), (c) and (d) is quite similar to that in the paper by Erickson, Semenoff and Zarembo [21], where their cancellation was explicitly shown

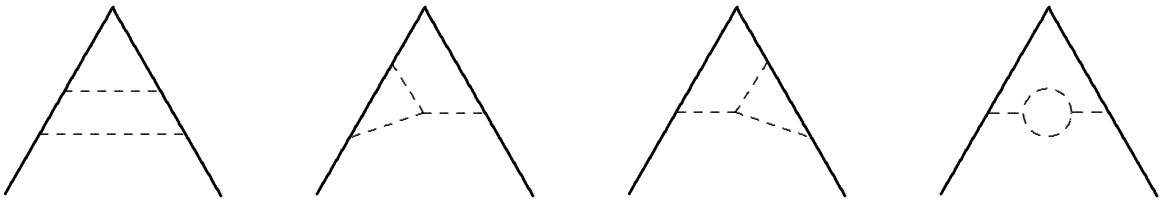

Figure 2: Two-loop diagrams relevant for the calculation of the anomalous dimension of the cusped Wilson loop. The dashed lines represent either the Yang-Mills or scalar propagators.

for straight and circular Wilson loops.

From Eqs. (13) and (14) of Ref. [21], the sum of all graphs with one internal three-point vertex in Figs. 2(b) and (c) is

$$\Sigma_3 = -\frac{\lambda^2}{4}\oint d\tau_1 d\tau_2 d\tau_3\, \epsilon(\tau_1\tau_2\tau_3)\left(|\dot{x}^{(1)}||\dot{x}^{(3)}| - \dot{x}^{(1)}\cdot\dot{x}^{(3)}\right)\dot{x}^{(2)}\cdot\frac{\partial}{\partial x^{(1)}}G(x^{(1)}x^{(2)}x^{(3)}) \tag{2.3}$$

where $\epsilon(\tau_1\tau_2\tau_3)$ performs antisymmetrization of τ_1, τ_2 and τ_3 and the scalar three-point function is

$$\begin{aligned} G(x^{(1)}x^{(2)}x^{(3)}) &= \int d^{2\omega}w\Delta(x^{(1)}-w)\Delta(x^{(2)}-w)\Delta(x^{(3)}-w) \\ &= \frac{\Gamma(2\omega-3)}{64\pi^{2\omega}}\int\frac{d\alpha d\beta d\gamma(\alpha\beta\gamma)^{\omega-2}\delta(1-\alpha-\beta-\gamma)}{\left[\alpha\beta|x^{(1)}-x^{(2)}|^2+\beta\gamma|x^{(2)}-x^{(3)}|^2+\gamma\alpha|x^{(3)}-x^{(1)}|^2\right]^{2\omega-3}}\,. \end{aligned} \tag{2.4}$$

Here, we will use a cut cusped trajectory in Euclidean space,

$$x^\mu(\tau) = \begin{cases} (\tau,0,0,0) & -L<\tau<-\varepsilon \quad \text{segment I} \\ (\tau\cos\theta,\tau\sin\theta,0,0) & \varepsilon<\tau<L \quad \text{segment II} \end{cases}, \tag{2.5}$$

where we must eventually put $L\to\infty$ and $\varepsilon\to 0$. We are computing a dimensionless quantity which can only depend on these in the ratio ε/L.

Because of the presence of $\left(|\dot{x}^{(1)}||\dot{x}^{(3)}| - \dot{x}^{(1)}\cdot\dot{x}^{(3)}\right)$ in the vertex, it vanishes unless τ_1 and τ_3 are on different segments.

There are four different cases for the integration:

$$\begin{aligned} &i) \qquad -\frac{\lambda^2}{4}(1-\cos\theta)\int_{-L}^{-\varepsilon}d\tau_1\int_{-L}^{-\varepsilon}d\tau_2\int_{\varepsilon}^{L}d\tau_3\epsilon(\tau_1\tau_2)\dot{x}^{(2)}\cdot\frac{\partial}{\partial x^{(1)}}\ldots \\ &ii) \qquad -\frac{\lambda^2}{4}(1-\cos\theta)\int_{-L}^{-\varepsilon}d\tau_1\int_{\varepsilon}^{L}d\tau_2\int_{\varepsilon}^{L}d\tau_3\epsilon(\tau_2\tau_3)\dot{x}^{(2)}\cdot\frac{\partial}{\partial x^{(1)}}\ldots \end{aligned}$$

$$
\begin{aligned}
iii) \qquad & -\frac{\lambda^2}{4}(1-\cos\theta)\int_\varepsilon^L d\tau_1\int_{-L}^{-\varepsilon} d\tau_2\int_{-\varepsilon}^{-L} d\tau_3\epsilon(\tau_2\tau_3)\dot{x}^{(2)}\cdot\frac{\partial}{\partial x^{(1)}}\ldots \\
iv) \qquad & -\frac{\lambda^2}{4}(1-\cos\theta)\int_\varepsilon^L d\tau_1\int_{\varepsilon}^{L} d\tau_2\int_{-\varepsilon}^{-L} d\tau_3\epsilon(\tau_1\tau_2)\dot{x}^{(2)}\cdot\frac{\partial}{\partial x^{(1)}}\ldots
\end{aligned}
\tag{2.6}
$$

In case $ii)$, differentiating the expression under the Feynman parameter integral in $\ldots$ leads to

$$
\begin{aligned}
&\dot{x}^{(2)}\cdot\frac{\partial}{\partial x^{(1)}}\frac{1}{\left[\alpha\beta|x^{(1)}-x^{(2)}|^2+\beta\gamma|x^{(2)}-x^{(3)}|^2+\gamma\alpha|x^{(3)}-x^{(1)}|^2\right]^{2\omega-3}} \\
&= \frac{-(2\omega-3)\left(2\alpha\beta(\tau_1\cos\theta-\tau_2)+2\alpha\gamma(\tau_1\cos\theta-\tau_3)\right)}{\left[\alpha\beta(\tau_1^2+\tau_2^2-2\tau_1\tau_2\cos\theta)+\beta\gamma(\tau_2-\tau_3)^2+\gamma\alpha(\tau_3^2+\tau_1^2-2\tau_3\tau_1\cos\theta)\right]^{2\omega-2}}\,.
\end{aligned}
\tag{2.7}
$$

We observe that the rest of the integrand is completely antisymmetric under interchange of τ_2,β and τ_3,γ whereas this term is symmetric. Therefore the integral must vanish, $ii)=0$. By a similar argument, $iii)=0$.

It remains to study $i)$ and $iv)$. There τ_1 and τ_2 are on the same segment of the contour and $\dot{x}^{(2)}\cdot\frac{\partial}{\partial x^{(1)}}=\frac{\partial}{\partial\tau_1}$. Integrating by parts produces a delta function and a surface term. Let us first study the term with a delta function. Using the delta function to integrate τ_2 results in

$$
\begin{aligned}
i) \qquad & \frac{\lambda^2}{2}(1-\cos\theta)\int_{-L}^{-\varepsilon} d\tau_1\int_\varepsilon^L d\tau_3\frac{\Gamma(2\omega-3)}{64\pi^{2\omega}}\int d\alpha d\beta d\gamma\frac{(\alpha\beta\gamma)^{\omega-2}\delta(1-\alpha-\beta-\gamma)}{\left[\gamma(1-\gamma)|x^{(1)}-x^{(3)}|^2\right]^{2\omega-3}} \\
iv) \qquad & \frac{\lambda^2}{2}(1-\cos\theta)\int_{\varepsilon}^L d\tau_1\int_{-\varepsilon}^{-L} d\tau_3\frac{\Gamma(2\omega-3)}{64\pi^{2\omega}}\int d\alpha d\beta d\gamma\frac{(\alpha\beta\gamma)^{\omega-2}\delta(1-\alpha-\beta-\gamma)}{\left[\gamma(1-\gamma)|x^{(1)}-x^{(3)}|^2\right]^{2\omega-3}}\,.
\end{aligned}
\tag{2.8}
$$

The result of doing the Feynman parameter integral in each case is

$$
i) \quad \frac{\lambda^2}{2}(1-\cos\theta)\int_{-L}^{-\varepsilon} d\tau_1\int_\varepsilon^L d\tau_3\frac{\Gamma(2\omega-3)}{64\pi^{2\omega}}\frac{\Gamma^2(\omega-1)}{(2-\omega)\Gamma(2\omega-2)}\frac{1}{\left[|x^{(1)}-x^{(3)}|^2\right]^{2\omega-3}}\,, \tag{2.9}
$$

$$
iv) \quad \frac{\lambda^2}{2}(1-\cos\theta)\int_{\varepsilon}^L d\tau_1\int_{-\varepsilon}^{-L} d\tau_3\frac{\Gamma(2\omega-3)}{64\pi^{2\omega}}\frac{\Gamma^2(\omega-1)}{(2-\omega)\Gamma(2\omega-2)}\frac{1}{\left[|x^{(1)}-x^{(3)}|^2\right]^{2\omega-3}}\,. \tag{2.10}
$$

The sum of all self-energy contributions to the Wilson loop is given by (from Eq. (12) of Ref. [21])

$$
\Sigma_2=-\frac{\lambda^2\Gamma^2(\omega-1)}{2^7\pi^{2\omega}(2-\omega)(2\omega-3)}\oint d\tau_1 d\tau_2\frac{|\dot{x}^{(1)}||\dot{x}^{(2)}|-\dot{x}^{(1)}\cdot\dot{x}^{(2)}}{\left[(x^{(1)}-x^{(2)})^2\right]^{2\omega-3}}\,. \tag{2.11}
$$

It is easy to see that this contribution is canceled by the sum of the two terms in Eqs. (2.9) and (2.10).

Thus, there remains only two contributions, the two surface terms which are obtained from the integration by parts:

$$
\begin{aligned}
i) \qquad & -\frac{\lambda^2}{4}(1-\cos\theta)\int_{-L}^{-\epsilon} d\tau_1 \int_{-L}^{-\varepsilon} d\tau_2 \int_{\varepsilon}^{L} d\tau_3 \frac{\partial}{\partial\tau_1}\left(\varepsilon(\tau_1\tau_2)G(x^{(1)},x^{(2)},x^{(3)})\right) \\
& \quad = -\frac{\lambda^2}{4}(1-\cos\theta)\int_{-L}^{-\varepsilon} d\tau_2 \int_{\varepsilon}^{L} d\tau_3 \left(-G(-\varepsilon,x^{(2)},x^{(3)}) - G(-L,x^{(2)},x^{(3)})\right) \\
iv) \qquad & -\frac{\lambda^2}{4}(1-\cos\theta)\int_{\varepsilon}^{L} d\tau_1 \int_{\varepsilon}^{L} d\tau_2 \int_{-\varepsilon}^{-L} d\tau_3 \frac{\partial}{\partial\tau_1}\left(\epsilon(\tau_1\tau_2)G(x^{(1)},x^{(2)},x^{(3)})\right) \\
& \quad = -\frac{\lambda^2}{4}(1-\cos\theta)\int_{\varepsilon}^{L} d\tau_2 \int_{-L}^{-\varepsilon} d\tau_3 \left(-G(L,x^{(2)},x^{(3)}) - G(\varepsilon,x^{(2)},x^{(3)})\right).
\end{aligned}
\tag{2.12}
$$

These integrals are doubly cutoff, by dimensional regularization and by ε and L. Now that we have canceled the singularity in the bubble diagram, it is safe to remove one of the regulators. Here we choose to remove the dimensional regulator to go to the physical dimension $\omega = 2$. In that case, we have

$$
\begin{aligned}
& G(x^{(1)}x^{(2)}x^{(3)}) \\
& \quad = \quad \frac{1}{64\pi^4}\int d\alpha d\beta d\gamma \frac{\delta(1-\alpha-\beta-\gamma)}{[\alpha\beta(x^{(1)}-x^{(2)})^2+\beta\gamma(x^{(2)}-x^{(3)})^2+\gamma\alpha(x^{(3)}-x^{(1)})^2]}.
\end{aligned}
\tag{2.13}
$$

Then, we find for the two surface terms

$$
\begin{aligned}
i) \qquad & = \frac{\lambda^2}{4}(1-\cos\theta)\int_{-L/\varepsilon}^{-1} d\tau_2 \int_{1}^{L/\varepsilon} d\tau_3 \left(G(-1,x^{(2)},x^{(3)}) + G(-L/\varepsilon,x^{(2)},x^{(3)})\right) \\
iv) \qquad & = \frac{\lambda^2}{4}(1-\cos\theta)\int_{1}^{L/\varepsilon} d\tau_2 \int_{-L/\epsilon}^{-1} d\tau_3 \left(G(L/\varepsilon,x^{(2)},x^{(3)}) + G(1,x^{(2)},x^{(3)})\right).
\end{aligned}
\tag{2.14}
$$

It is clear that the divergence in these integrals is like log, not $\log^2$. The logarithmically divergent part is gotten by taking a derivative $\varepsilon\frac{d}{d\varepsilon}$. After that, the τ-integrations reduce to one remaining integration. Also remaining are the Feynman parameters. The sum of the logarithmic terms is given by

$$
-2\ln(\varepsilon/L)\int_0^1 \frac{d\alpha d\beta d\gamma d\tau\,\delta(1-\alpha-\beta-\gamma)}{\gamma(1-\gamma)\tau^2+2\cos\theta\beta\gamma\tau+\beta(1-\beta)}\,. \tag{2.15}
$$

We can use a symmetry of the integral under $\tau \to 1/\tau$ and interchanging γ and β to write it as

$$
-\ln(\varepsilon/L)\int_0^\infty d\tau \int_0^1 \frac{d\alpha d\beta d\gamma\,\delta(1-\alpha-\beta-\gamma)}{\gamma(1-\gamma)\tau^2+2\cos\theta\beta\gamma\tau+\beta(1-\beta)}\,. \tag{2.16}
$$

Finally, we obtain

$$
\gamma_{\rm cusp}^{(b)+(c)+(d)} = -\frac{\lambda^2}{64\pi^4} I \tag{2.17}
$$

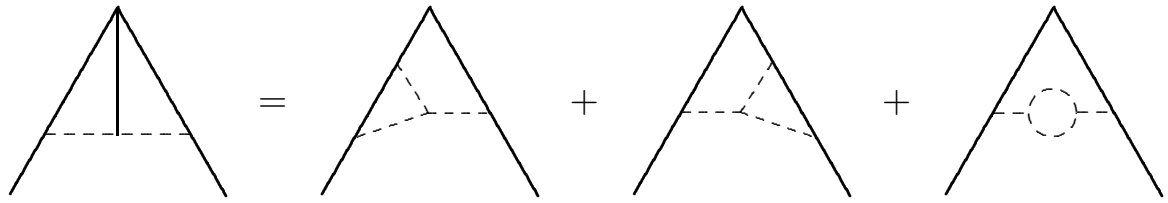

Figure 3: Two-loop anomaly diagram (a) which emerges as a surface term in the sum of the diagrams (b), (c) and (d). An analytic expression is given by the sum of $i)$ and $iv)$ in Eq. (2.14).

with

$$I = (\cos\theta - 1)\int_0^\infty d\tau \int_0^1 \frac{d\alpha d\beta d\gamma\, \delta(1-\alpha-\beta-\gamma)}{\gamma(1-\gamma)\tau^2 + 2\cos\theta\beta\gamma\tau + \beta(1-\beta)} \tag{2.18}$$

for the contribution of the two loop diagrams in Figs. $2(b)$, (c) and (d) to the cusp anomalous dimension.

It is worth noting once again that Eqs. (2.17) and (2.18) result from the surface term which would be missing if there were no cusp and the loop were smooth. This can be easily seen from Eq. (2.18) since I vanishes for $\theta = 0$.

It is convenient to depict the sum of the two-loop diagrams (b), (c) and (d) as the anomalous diagram in Fig. $3(a)$. All three propagators in Fig. $3(a)$ are scalar as it follows from Eqs. (2.14) and (2.13). We shall call this as the anomalous term.

3 Cusp anomalous dimension at two loops

As we have explained in the Introduction, we are interested in the cusp anomalous dimension for large angle θ in Minkowski space. The analytic continuation of Eq. (2.18) to Minkowski space can easily be done by passing to the Minkowski variable (2.2) by the analytic continuation $\theta \to \mathrm{i}\theta$. The result is to replace $\cos\theta$ where it appears in Eq. (2.18) by $\cosh\theta$.

3.1 Arbitrary θ

Introducing the variables

$$\tilde\beta = \frac{1}{\beta} - 1, \quad 0 < \tilde\beta < \infty\,; \qquad \beta = \frac{1}{1+\tilde\beta} \tag{3.1}$$

and

$$\tilde z = \frac{1}{\gamma\beta} - \frac{1}{\gamma} - \frac{1}{\beta}, \quad 0 < \tilde z < \infty\,; \qquad \gamma = \frac{\tilde\beta}{1+\tilde z+\tilde\beta} \tag{3.2}$$

we rewrite the integral in Eq. (2.18) as

$$\begin{aligned} I &= (\cosh\theta - 1)\int_0^\infty d\tau \int_0^1 d\beta \int_0^{1-\beta} d\gamma \frac{1}{\gamma(1-\gamma)\tau^2 + 2\gamma\beta\cosh\theta\tau + \beta(1-\beta)} \\ &= (\cosh\theta - 1)\int_0^\infty d\tilde{\tau} \int_1^\infty dz \frac{1}{z\tilde{\tau}^2 + 2\cosh\theta\tilde{\tau} + 1} \int_0^\infty \frac{d\tilde{\beta}}{(\tilde{\beta}+1)(\tilde{\beta}+z)} \\ &= (\cosh\theta - 1)\int_1^\infty \frac{dz \ln z}{(z-1)\sqrt{\cosh^2\theta - z}} \ln \frac{\cosh\theta + \sqrt{\cosh^2\theta - z}}{\sqrt{z}} \end{aligned} \tag{3.3}$$

with

$$z = \tilde{z} + 1\,, \qquad \tilde{\tau} = \frac{(\tilde{\beta}+1)}{(\tilde{\beta}+z)}\tau\,. \tag{3.4}$$

The integrand on the right-hand side of Eq. (3.3) is real both of the regions $z < \cosh^2\theta$ and $z > \cosh^2\theta$. The integral is convergent as $z \to 1$ or $z \to \infty$.

It is convenient to change the variable z in the integral on the right-hand side of Eq. (3.3) to the angular variable

$$\psi = \ln \frac{\cosh\theta + \sqrt{\cosh^2\theta - z}}{\sqrt{z}}, \qquad z = \frac{\cosh^2\theta}{\cosh^2\psi}. \tag{3.5}$$

The variable ψ decreases from θ to 0 when z increases from 1 to $\cosh^2\theta$ and then runs along the imaginary axis from 0 to $\mathrm{i}\pi/2$ when z further increases from $\cosh^2\theta$ to ∞. We thus rewrite the integral as

$$I = 4\frac{\cosh\theta - 1}{\cosh\theta}\left(\int_0^\theta + \int_0^{\pi/2}\right)\frac{d\psi\,\psi}{1 - \cosh^2\psi/\cosh^2\theta} \ln\frac{\cosh\theta}{\cosh\psi}. \tag{3.6}$$

3.2 Large θ

The asymptotics at large θ of the first integral in Eq. (3.6) is governed by

$$4\int_0^\theta \frac{d\psi\psi(\theta-\psi)}{1 - \mathrm{e}^{\,2(\psi-\theta)}} = 4\int_0^\theta d\psi\psi(\theta-\psi)\left(1 + \sum_{n=1}^\infty \mathrm{e}^{\,-2n(\theta-\psi)}\right). \tag{3.7}$$

Noting that only the values of $(\theta - \psi) \sim 1$ are essential in the integral in each term of the sum over $n \geq 1$ in Eq. (3.7) at large θ with an exponential in θ accuracy, we obtain asymptotically

$$\begin{aligned} 4\left(\frac{1}{6}\theta^3 + \theta\sum_{n=1}^\infty \frac{1}{4n^2}\right) &= 4\left(\frac{1}{6}\theta^3 + \frac{\zeta(2)}{4}\theta + \mathcal{O}(1)\right) \\ &= \frac{2}{3}\theta^3 + \frac{\pi^2}{6}\theta + \mathcal{O}(1)\,. \end{aligned} \tag{3.8}$$

A term which is linear in θ also comes from the second integral in Eq. (3.6). For large θ the latter takes the form

$$4\int_0^{\pi/2} d\psi\,\psi\theta = \frac{\pi^2}{2}\theta\,. \tag{3.9}$$

Summing the asymptotics (3.8) and (3.9), we find, the contributions of the sum of the diagrams in Figs. 2(b), (c) and (d):

$$\gamma_{\rm cusp}^{(b)+(c)+(d)} = -\frac{\lambda^2}{96\pi^4}\left(\theta^3+\pi^2\theta+\mathcal{O}(1)\right). \tag{3.10}$$

3.3 Adding the ladder diagram

The expansion of Eq. (3.10) in large θ begins from a term of order θ^3. This term cancels the one coming from the ladder diagram in Fig. 2(l). It is convenient to add and subtract the diagram with crossed propagator lines. After that, the sum exponentiates the contribution of the order λ. The remaining contribution is proportional to the one calculated in Ref. [3] and reads as

$$\gamma_{\rm cusp}^{(l)} = \frac{\lambda^2}{128\pi^4}\frac{(\cosh\theta-1)^2}{\sinh^2\theta}\int_0^\infty\frac{d\sigma}{\sigma}\ln\left(\frac{1+\sigma\,{\rm e}^{\,\theta}}{1+\sigma\,{\rm e}^{\,-\theta}}\right)\ln\left(\frac{\sigma+\,{\rm e}^{\,\theta}}{\sigma+\,{\rm e}^{\,-\theta}}\right). \tag{3.11}$$

This integral possesses the symmetry $\sigma\to 1/\sigma$ which makes it equal twice the integral from 0 to 1.

Introducing the angular variable

$$\psi = \frac{1}{2}\ln\frac{1+\sigma\,{\rm e}^{\,\theta}}{1+\sigma\,{\rm e}^{\,-\theta}} \tag{3.12}$$

and noting that

$$\frac{d\sigma}{\sigma} = d\psi\,[\coth\psi+\coth(\theta-\psi)]\,, \tag{3.13}$$

we rewrite the integral in Eq. (3.11) as

$$\begin{aligned}\frac{\lambda^2}{16\pi^4}\frac{(\cosh\theta-1)^2}{\sinh^2\theta}&\int_0^\theta d\psi\psi(\theta-\psi)\coth\psi\\ &=\frac{\lambda^2}{16\pi^4}\frac{(\cosh\theta-1)^2}{\sinh^2\theta}\int_0^\theta d\psi\psi(\theta-\psi)\left(1+2\sum_{n=1}^\infty{\rm e}^{\,-2n\psi}\right)\end{aligned} \tag{3.14}$$

whose asymptotics at large θ is

$$\gamma_{\rm cusp}^{(l)} = \frac{\lambda^2}{16\pi^4}\left(\frac{\theta^3}{6}+\frac{\zeta(2)}{2}\theta+\mathcal{O}(1)\right) = \frac{\lambda^2}{96\pi^4}\left(\theta^3+\frac{\pi^2}{2}\theta+\mathcal{O}(1)\right). \tag{3.15}$$

Summing up the contributions of all of the four diagrams in Fig. 2, we finally obtain

$$\gamma_{\rm cusp} = \frac{\theta}{2}\left(\frac{\lambda}{2\pi^2}-\frac{\lambda^2}{96\pi^2}\right)+\mathcal{O}(\theta^0) \tag{3.16}$$

for the cusp anomalous dimension to order λ^2. This expression agrees with the result in Eq. (1.5) which is obtained by different methods.

4 Cusped loop equation to order λ^2

The dynamics of Wilson loops in Yang-Mills theory is governed by the loop equation [34] (for details see Ref. [1], Chapter 12). An extension of the loop equation to $\mathcal{N}=4$ SYM was proposed by Drukker, Gross and Ooguri [17]. It deals with supersymmetric loops $\boldsymbol{C}=\{x_\mu(\sigma),Y_i(\sigma);\zeta(\sigma)\}$, where $\zeta(\sigma)$ denotes the Grassmann odd component.

For cusped Wilson loops this loop equation reads as

$$\begin{aligned}\boldsymbol{\Delta}\ln W(\boldsymbol{C})\Big|_{\boldsymbol{C}=\Gamma} &= \lambda\int \mathrm{d}\sigma_1\int \mathrm{d}\sigma_2\ (\dot{x}_\mu(\sigma_1)\dot{x}_\mu(\sigma_2)-|\dot{x}_\mu(\sigma_1)||\dot{x}_\mu(\sigma_2)|)\\ &\quad\times\delta^{(4)}(x_1-x_2)\frac{W(\Gamma_{x_1x_2})W(\Gamma_{x_2x_1})}{W(\Gamma)}\,,\end{aligned}\tag{4.1}$$

where

$$\boldsymbol{\Delta}=\lim_{\eta\to0}\int \mathrm{d}s\int_{s-\eta}^{s+\eta}\mathrm{d}s'\left(\frac{\delta^2}{\delta x^\mu(s')\delta x_\mu(s)}+\frac{\delta^2}{\delta Y^i(s')\delta Y_i(s)}+\frac{\delta^2}{\delta\zeta(s')\delta\bar{\zeta}(s)}\right)\tag{4.2}$$

is the supersymmetric extension of the loop-space Laplacian and we put $\dot{Y}^2=\dot{x}^2$, $\zeta=0$ after acting by $\boldsymbol{\Delta}$. The coefficient on the right-hand side of Eq. (4.1) accounts for the fact that the Wilson loops are in the adjoint representation.

Equation (4.1) is in the spirit of the general form of the loop equation applicable for scalar theory [35]. For later convenience the operator on the left-hand side acts on $\ln W$ rather than on W itself and, correspondingly, the right-hand side is divided by $W(\Gamma)$. This is possible because $\boldsymbol{\Delta}$ is an operator of first order (obeys the Leibnitz rule). A different but equivalent operator was used in Ref. [36] for deriving loop equations in the IIB matrix model.

It was argued in Ref. [33] that an infinite straight Wilson line is a solution of the $\mathcal{N}=4$ SYM loop equation. In Ref. [17] it was shown to order λ that the right-hand side of the cusped loop equation is proportional to the cusped anomalous dimension, when the presence of $W(\Gamma)$ in the denominator was not essential to order λ since $W=1+\mathcal{O}(\lambda)$. We shall demonstrate in this Section that this also works for the cusped loop equation (4.1) to the order λ^2.

4.1 The set up

The delta-function on the right-hand side of Eq. (4.1) has to be regularized consistently with the UV regularization of the propagator, *e.g.*

$$D_a(x)=\frac{1}{4\pi^2(x^2+a^2)}\,,\qquad \delta_a^{(4)}(x)=\frac{2a^2}{\pi^2(x^2+a^2)^3}\,,\tag{4.3}$$

where a is a UV cutoff.

In contrast to the usual Yang-Mills loop equation [34], the term of the order L/a^3 on the right-hand side of Eq. (4.1) coming from the Yang-Mills field is canceled by scalars.

For smooth loops the right-hand side of Eq. (4.1) will be of the order $(La)^{-1}$ where L is a typical size of the loop. Analogously, the operator $\mathbf{\Delta}$ on the left-hand side will produce a term of the same order. The situation changes for cusped Wilson loops, when the right-hand side is estimated to be of the order a^{-2} which is much larger. So the loop equation has specific features for cusped loops. We are thus going to verify Eq. (4.1) at the order a^{-2}.

An analysis of diagrams with the regularized propagator (4.3) suggests that the action of the loop-space Laplacian Δ on each diagram can be replaced for the cusped Wilson loops to the order a^{-2} by a differentiation with respect to a:

$$\Delta \ln W(C)\Big|_{C=\Gamma} = 2\left(\frac{1}{a}\frac{\mathrm{d}}{\mathrm{d}a} - \frac{\mathrm{d}^2}{\mathrm{d}a^2}\right)\ln W(\Gamma) + \mathcal{O}\left(a^{-1}\right) . \tag{4.4}$$

This prescription follows from the formula

$$-2\left(\frac{1}{a}\frac{\mathrm{d}}{\mathrm{d}a} - \frac{\mathrm{d}^2}{\mathrm{d}a^2}\right) D_a(x) = \delta_a^{(4)}(x) \tag{4.5}$$

and it can be shown for the diagrams of the orders λ and λ^2.

We therefore conjecture that

$$\mathbf{\Delta} \ln W(\boldsymbol{C})\Big|_{\boldsymbol{C}=\Gamma} = \frac{2}{a^2}\gamma_{\mathrm{cusp}}\left(\theta,\lambda\right) + \mathcal{O}\left(a^{-1}\right) \tag{4.6}$$

so that Eq. (4.1) reduces to

$$\begin{aligned}\frac{2}{a^2}\gamma_{\mathrm{cusp}}\left(\theta,\lambda\right) \;&=\; \lambda\int \mathrm{d}\sigma_1 \int \mathrm{d}\sigma_2 \;\left(\dot{x}_\mu(\sigma_1)\dot{x}_\mu(\sigma_2) - |\dot{x}_\mu(\sigma_1)||\dot{x}_\mu(\sigma_2)|\right) \\ &\qquad \times \delta_a^{(4)}(x_1 - x_2)\frac{W(\Gamma_{x_1x_2})W(\Gamma_{x_2x_1})}{W(\Gamma)}\end{aligned} \tag{4.7}$$

for the cusped Wilson loops to the order a^{-2}. We shall verify Eq. (4.7) to the order λ^2 by calculating the right-hand side.

To the order λ the ratio of the W's on the right-hand side of Eq. (4.1) equals 1, and we have

$$\begin{aligned}&\lambda\int \mathrm{d}\sigma_1 \int \mathrm{d}\sigma_2 \;\left(\dot{x}_\mu(\sigma_1)\dot{x}_\mu(\sigma_2) - |\dot{x}_\mu(\sigma_1)||\dot{x}_\mu(\sigma_2)|\right)\delta_a^{(4)}(x_1 - x_2) \\ &\quad = 2\lambda(\cosh\theta - 1)\int_0^\infty \mathrm{d}S \int_0^\infty \mathrm{d}T\, \frac{2a^2}{\pi^2(S^2 + 2ST\cosh\theta + T^2 + a^2)^3} .\end{aligned} \tag{4.8}$$

Changing the variables for the radial variable r and the angular variable ν:

$$S = \frac{\sqrt{r}}{\sqrt{\nu^2 + 2\nu\cosh\theta + 1}} , \qquad T = \frac{\nu\sqrt{r}}{\sqrt{\nu^2 + 2\nu\cosh\theta + 1}} , \tag{4.9}$$

we rewrite Eq. (4.8) as

$$\begin{aligned}&\frac{2}{\pi^2}\lambda(\cosh\theta - 1)\int_0^\infty \mathrm{d}r\, \frac{a^2}{(r + a^2)^3}\int_0^\infty \mathrm{d}\nu\, \frac{1}{\nu^2 + 2\nu\cosh\theta + 1} \\ &\quad = \frac{1}{2\pi^2 a^2}\lambda\frac{(\cosh\theta - 1)}{\sinh\theta}\theta\end{aligned} \tag{4.10}$$

which agrees with [17] and to the order λ reproduces (1.5) through Eq. (4.7).

4.2 Ladder contribution

To the order λ^2 we substitute on the right-hand side of Eq. (4.1) the ratio of the W's from the previous order λ, so that only (minus) the diagrams with crossed lines (one propagator line and one line representing $\delta_a^{(4)}(x_1 - x_2)$) are left after the cancellation. We obtain for the right-hand side

$$\begin{aligned}&\frac{1}{2}\lambda^2(\cosh\theta - 1)^2 \int_0^\infty \mathrm{d}S \int_0^\infty \mathrm{d}T \left(\int_0^S \mathrm{d}s \int_T^\infty \mathrm{d}t + \int_S^\infty \mathrm{d}s \int_0^T \mathrm{d}t \right) \\ &\quad \times \frac{2a^2}{\pi^2(S^2 + 2ST\cosh\theta + T^2 + a^2)^3} \frac{1}{4\pi^2(s^2 + 2st\cosh\theta + t^2 + a^2)} \end{aligned} \tag{4.11}$$

which gives after the separation of radial and angular variables

$$\begin{aligned}&\frac{\lambda^2}{2\pi^4}(\cosh\theta - 1)^2 \int_0^\infty \mathrm{d}r \, \frac{a^2}{(r + a^2)^3} \int_0^\infty \mathrm{d}\nu \, \frac{1}{\nu^2 + 2\nu\cosh\theta + 1} \\ &\quad \times \int_0^1 \mathrm{d}\sigma \int_\nu^\infty \mathrm{d}\tau \, \frac{1}{\sigma^2 + 2\sigma\tau\cosh\theta + \tau^2} \\ &= \frac{\lambda^2}{64\pi^4 a^2} \frac{(\cosh\theta - 1)^2}{\sinh^2\theta} \int_0^\infty \frac{\mathrm{d}\tilde{\nu}}{\tilde{\nu}} \ln\left(\frac{1 + \tilde{\nu}\,\mathrm{e}^{\,\theta}}{1 + \tilde{\nu}\,\mathrm{e}^{\,-\theta}} \right) \ln\left(\frac{\tilde{\nu} + \mathrm{e}^{\,\theta}}{\tilde{\nu} + \mathrm{e}^{\,-\theta}} \right), \end{aligned} \tag{4.12}$$

where we substituted

$$s = \sigma S\,, \qquad t = \tau S\,, \qquad \nu = \sigma\tilde{\nu}\,. \tag{4.13}$$

The expression on the right-hand side of Eq. (4.12) is the same as in Eq. (3.11).

4.3 Anomaly contribution

In order to find the contribution from the anomaly, we need to be more careful with the regularization. The regularization (4.3) violate, in general, the $\mathcal{N} = 4$ supersymmetry. We shall instead regularize by the standard dimensional reduction, which preserve the supersymmetry. Otherwise we cannot expect the cancellation described in Sect. 2.

However, the dimensional regularization does not properly regularize the delta-function on the right-hand side of Eq. (4.1). We shall introduce additionally the smearing of the delta-function by

$$\delta^{(d)}(x - y) \longrightarrow \int\limits_{\text{reg.}} \mathrm{d}\tau \, \frac{\partial}{\partial\tau} \frac{1}{(2\pi\tau)^{d/2}} \, \mathrm{e}^{\,-(x-y)^2/2\tau} \tag{4.14}$$

or in the form preserving gauge invariance by the path integral of the path-ordered exponential:

$$\delta^{(d)}(x - y) \longrightarrow \int\limits_{\text{reg.}} \mathrm{d}\tau \, \frac{\partial}{\partial\tau} \int\limits_{\substack{z(0)=x \\ z(\tau)=y}} \mathcal{D}z(t) \, \mathrm{e}^{\,-\int_0^\tau \mathrm{d}t\, \dot{z}^2(t)/2} \, \boldsymbol{P} \, \mathrm{e}^{\,\mathrm{i}\int_0^\tau \mathrm{d}t\, \dot{z}^\mu A_\mu(z)}\,. \tag{4.15}$$

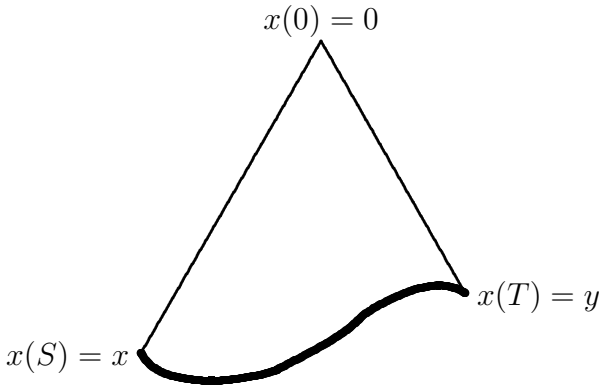

Figure 4: Typical path $z(t)$ (represented by the bold line) connecting $x = z(0)$ and $y = z(\tau)$ in the regularization of the delta-function on the right-hand side of the loop equation by Eq. (4.15). A typical length of the path is $\sim a$.

A typical path $z(t)$ connecting $x = z(0)$ and $y = z(\tau)$ in the regularization of the delta-function on the right-hand side of the loop equation (4.1) by the path integral (4.15) is depicted in Fig. 4 by the bold line. A typical length of this path is $\sim a$.

In Eqs. (4.14) and (4.15) the integral over the proper time τ is cut at $\tau \sim a^2$ with a being the UV cutoff. The regularization (4.3) is associated with

$$\int\limits_{\rm reg.} \cdots = \int_0^\infty {\rm e}^{\,-a^2/2\tau} \ \cdots \tag{4.16}$$

while the Schwinger proper-time regularization is given by

$$\int\limits_{\rm reg.} \cdots = \int_{a^2}^\infty \ \cdots \ . \tag{4.17}$$

Introducing a UV cutoff a on the right-hand side of the loop equation inevitably results in a UV regularization of propagators at distances $\sim a$. To preserve SUSY we choose a to be much smaller than the UV cutoff, provided by the dimensional regularization.

In order to calculate the right-hand side of the loop equation to the order λ^2, we need the Wilson loop average to the order λ. A nonvanishing contribution comes from the diagrams depicted in Figs. 5(a), (b) and (c). The diagram in Fig. 5(a) is the usual one, while for the diagrams (b) and (c) one end of the propagator line ends at the path regularizing the delta-function. The length of this path from x to y is $\sim \sqrt{\tau}$, which we do not consider to be small because the contribution of this diagram to the right-hand side of Eq. (4.1) will also be $\sim 1/a^2$ for $\tau \sim a^2$.

The diagram in Fig. 5(a) results in the ladder diagram which we have already considered in the previous subsection. The diagrams in Figs. 5(b) and (c) result in the anomaly diagram of type depicted in Fig. 6.

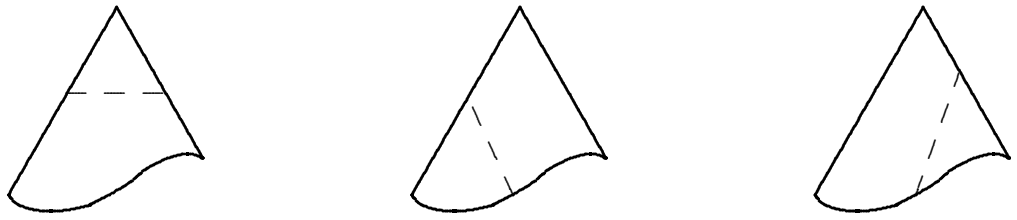

(a) (b) (c)

Figure 5: Diagrams of order λ for closed cusped Wilson loop. The diagram (a) is the usual one. For the diagrams (b) and (c) one end of the propagator line ends at the regularizing path.

The latter statement can be proved by virtue of the useful formula

$$\int\limits_{\substack{z(0)=x\\z(\tau)=y}} \mathcal{D}z(t)\,\mathrm{e}^{-\int_0^\tau \mathrm{d}t\,\dot{z}^2(t)/2}\int_x^y \mathrm{d}z^\mu\delta^{(d)}(z-u) = \frac{1}{2}\int_0^\infty \mathrm{d}\tau_1\int_0^\infty \mathrm{d}\tau_2\,\delta\left(\tau-\tau_1-\tau_2\right)$$
$$\times\frac{1}{(2\pi\tau_1)^{d/2}}\,\mathrm{e}^{-(x-u)^2/2\tau_1}\frac{\overleftrightarrow{\partial}}{\partial u_\mu}\frac{1}{(2\pi\tau_2)^{d/2}}\,\mathrm{e}^{-(y-u)^2/2\tau_2} \tag{4.18}$$

which can be derived using the technique of Ref. [37][4]. The geometry is shown in Fig. 6. The anomaly diagram in Fig. 6 then appears by the same token as in Sect. 2. We believe that it also works for the regularization

$$\delta^{(d)}(x-y) \longrightarrow \int\limits_{\text{reg.}} \mathrm{d}\tau\,\frac{\partial}{\partial\tau}\int\limits_{\substack{z(0)=x\\z(\tau)=y}} \mathcal{D}z(t)\,\mathrm{e}^{-\int_0^\tau \mathrm{d}t\,\dot{z}^2(t)/2}\,\boldsymbol{P}\,\mathrm{e}^{\,\mathrm{i}\int_0^\tau \mathrm{d}t\left(\dot{z}^\mu A_\mu(z)+|\dot{z}|n^i\Phi_i(z)\right)} \tag{4.19}$$

which is both gauge-invariant and supersymmetric.

The contribution of the anomaly diagram in Fig. 6 to the right-hand side of Eq. (4.1) is given by

$$\begin{aligned}
&\frac{\lambda^2}{4}\int_0^\infty \mathrm{d}S\int_0^\infty \mathrm{d}T\,\left(\dot{x}_\mu(S)\dot{x}_\mu(T)-|\dot{x}(S)||\dot{x}(T)|\right)\int\limits_{\text{reg.}}\mathrm{d}\tau\,\frac{\partial}{\partial\tau}\int_0^\infty \mathrm{d}\tau_1\int_0^\infty \mathrm{d}\tau_2\int_0^\infty \mathrm{d}\tau_3\\
&\quad\times\delta\left(\tau-\tau_1-\tau_2\right)\int \mathrm{d}^d u\,\frac{\mathrm{e}^{-(x-u)^2/2\tau_1}}{(2\pi\tau_1)^{d/2}}\,\frac{\mathrm{e}^{-(y-u)^2/2\tau_2}}{(2\pi\tau_2)^{d/2}}\,\frac{\mathrm{e}^{-u^2/2\tau_3}}{(2\pi\tau_3)^{d/2}}\\
&=-\frac{\lambda^2}{4(2\pi)^d}\left(\cosh\theta-1\right)\Gamma(2\omega-1)\int_0^\infty \mathrm{d}S\int_0^\infty \mathrm{d}T\\
&\quad\times\int_0^1\frac{\mathrm{d}\alpha\,\mathrm{d}\beta\,\mathrm{d}\gamma\,(\alpha\beta\gamma)^{\omega-2}\delta(1-\alpha-\beta-\gamma)\beta^2\gamma^2/(\beta+\gamma)^2}{[\beta(1-\beta)S^2+2\cosh\theta\beta\gamma ST+\gamma(1-\gamma)T^2+a^2\beta^2\gamma^2/(\beta+\gamma)^2]^{2\omega-1}}\,,
\end{aligned} \tag{4.20}$$

[4]See also Ref. [1], pp. 32–33.

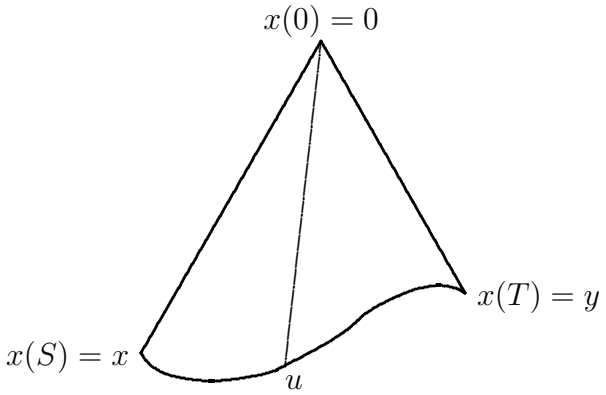

Figure 6: Two-loop anomaly diagram on the right-hand side of the loop equation (4.1). An analytic expression is given by Eq. (4.20).

where $x(S) = x$, $x(T) = y$ and $x(0) = 0$ and we have used the regularization (4.16).

The integral on the right-hand side of Eq. (4.20) can be treated similarly to Eq. (3.3). Introducing the radial variable r and the angular variable ν by

$$\begin{aligned} T &= \frac{\sqrt{r}}{\sqrt{\gamma(1-\gamma)\nu^2 + 2\beta\gamma\nu\cosh\theta + \beta(1-\beta)}}\,, \\ S &= \frac{\nu\sqrt{r}}{\sqrt{\gamma(1-\gamma)\nu^2 + 2\beta\gamma\nu\cosh\theta + \beta(1-\beta)}}\,, \end{aligned} \tag{4.21}$$

we find in $d = 4$

$$\begin{aligned} \text{Eq. (4.20)} &= -\frac{\lambda^2}{64\pi^2}(\cosh\theta - 1)\int_0^\infty \mathrm{d}\nu \\ &\times \int_0^1 \frac{\mathrm{d}\alpha\,\mathrm{d}\beta\,\mathrm{d}\gamma\,\delta(1-\alpha-\beta-\gamma)\beta^2\gamma^2/(\beta+\gamma)^2}{\gamma(1-\gamma)\nu^2 + 2\beta\gamma\nu\cosh\theta + \beta(1-\beta)} \int_0^\infty \mathrm{d}r \frac{a^2}{(r + a^2\beta^2\gamma^2/(\beta+\gamma)^2)^3} \\ &= -\frac{\lambda^2}{32\pi^2 a^2}(\cosh\theta - 1)\int_1^\infty \frac{\mathrm{d}z\,\ln z}{(z-1)\sqrt{\cosh^2\theta - z}} \ln\frac{\cosh\theta + \sqrt{\cosh^2\theta - z}}{\sqrt{z}}\,. \end{aligned} \tag{4.22}$$

This is the same integral as in Eq. (3.3)

5 Ladder diagrams

Summing the ladder diagrams is the simplest way to go beyond perturbation theory. They belong to the class of rainbow diagrams whose important role in the AdS/CFT correspondence is already recognized [21]. For the cusped Wilson loop depicted in Fig. 1, the ladder and rainbow diagrams are essentially the same because the rainbow diagrams vanish if a propagator has the ends at the same ray of the loop.

Our idea will be to sum up the ladder diagrams for the cusped SYM Wilson loop, and to investigate whether or not they can reproduce the $\sqrt{\lambda}$-behavior of the cusp anomalous dimension at large λ. This is motivated by the results of Ref. [20] for the sum of the ladder diagrams in the case of antiparallel Wilson lines.

5.1 The ladder equation

The Bethe-Salpeter equation for the sum of the ladder diagrams is similar to that of Ref. [20].

Let the parameter τ in Eq. (2.1) be: $\tau = t$ for $\tau > 0$ and $\tau = -s$ for $\tau < 0$. Let $s \in [a, S]$ and $t \in [b, T]$, i.e. a and b are lower limits for the integration over s and t, respectively. Correspondingly, S and T are the upper limits. We denote the sum of such defined ladder graphs as $G\,(S, T; a, b)$. It would play the role of a kernel in an exact Bethe-Salpeter equation, summing all diagrams not only ladders. In particular, it appears in the cusped loop equation (4.1).

It we pick up the first (closest to the cusp) rung of the ladder, we obtain the equation

$$G\,(S, T; a, b) = 1 - \frac{\lambda}{4\pi^2}(\cosh\theta - 1)\int_a^S ds \int_b^T dt\, \frac{G\,(S, T; s, t)}{s^2 + 2st\cosh\theta + t^2}\,. \tag{5.1}$$

It we alternatively pick up the last (farthest from the cusp) rung of the ladder, we get the equation

$$G\,(S, T; a, b) = 1 - \frac{\lambda}{4\pi^2}(\cosh\theta - 1)\int_a^S ds \int_b^T dt\, \frac{G\,(s, t; a, b)}{s^2 + 2st\cosh\theta + t^2}\,. \tag{5.2}$$

In order to find an iterative solution of the ladder equation, it is convenient first to account for exponentiation by introducing

$$F(S, T; a, b) = -\ln G(S, T; a, b)\,. \tag{5.3}$$

Then the ladder equation (5.2) takes the form (this can be shown by converting the equation for G to a differential equation, then substituting $G = e^{-F}$, then re-integrating)

$$\begin{aligned} F(S, T; a, b) \;&=\; \frac{\lambda}{4\pi^2}(\cosh\theta - 1)\int_a^S ds \int_b^T dt\, \frac{1}{s^2 + 2st\cosh\theta + t^2} \\ &\quad + \int_a^S ds \int_b^T dt\, \frac{\partial F(s, t; a, b)}{\partial s}\frac{\partial F(s, t; a, b)}{\partial t}\,. \end{aligned} \tag{5.4}$$

The order λ is given by the first term on the right-hand side and we obtain

$$\begin{aligned} F_1(S, T; a, b) \;&=\; \frac{\lambda}{4\pi^2}\frac{\cosh\theta - 1}{2\sinh\theta}\left(L_2(-\frac{T}{S}e^{\theta}) - L_2(-\frac{T}{S}e^{-\theta}) - L_2(-\frac{T}{a}e^{\theta}) + L_2(-\frac{T}{a}e^{-\theta})\right. \\ &\quad \left. - L_2(-\frac{b}{S}e^{\theta}) + L_2(-\frac{b}{S}e^{-\theta}) + L_2(-\frac{b}{a}e^{\theta}) - L_2(-\frac{b}{a}e^{-\theta})\right). \end{aligned} \tag{5.5}$$

Here L_2 is Euler's dilogarithm

$$L_2(z) = \sum_{n=1}^{\infty} \frac{z^n}{n^2} = -\int_0^z \frac{dx}{x}\, \ln(1-x) \tag{5.6}$$

which obeys the relation[5]

$$L_2\left(-e^{\Omega}\right) + L_2\left(-e^{-\Omega}\right) = -\frac{1}{2}\ln^2\Omega - \frac{\pi^2}{6}\,. \tag{5.7}$$

Using (5.7), it can be shown that Eq. (5.5) possesses a proper symmetry under interchange of S, a and T, b.

When $S = \infty$ four terms on the right-hand side of Eq. (5.5) vanish and we find

$$F_1(S=\infty, T; a, b\sim a) \overset{T\gg a}{=} \frac{\lambda}{4\pi^2}\frac{\cosh\theta - 1}{\sinh\theta}\,\theta \ln\frac{T}{a} \tag{5.8}$$

for $\ln(T/a) \gg 1$ and $a \sim b$.

The order λ^2 can be obtained by inserting F_1 into the second term on the right-hand side of Eq. (5.4). This gives

$$\begin{aligned} F_2(S,T;a,b) &= \frac{\lambda^2}{16\pi^4}(\cosh\theta - 1)^2 \int_a^S ds_1 \int_b^T dt_2 \\ &\quad \times \int_b^{t_2} \frac{dt_1}{(s_1^2 + 2\cosh\theta s_1 t_1 + t_1^2)} \int_a^{s_1} \frac{ds_2}{(s_2^2 + 2\cosh\theta s_2 t_2 + t_2^2)} \end{aligned} \tag{5.9}$$

which is nothing but the diagram with crossed ladders. This expression can be easily integrated twice.

By the differentiation of the result with respect to a and b, we get

$$\begin{aligned} &-a\frac{d}{da}F_2(S,T;a,b)\Big|_{S=T=\infty} \\ &\quad = \frac{\lambda^2}{16\pi^4}\left(\frac{\cosh\theta-1}{2\sinh\theta}\right)^2 \int_b^{\infty}\frac{dt}{t}\ln\left(\frac{a+t\,e^{\theta}}{a+t\,e^{-\theta}}\right)\ln\left(\frac{t+a\,e^{\theta}}{t+a\,e^{-\theta}}\right), \\ &-b\frac{d}{db}F_2(S,T;a,b)\Big|_{S=T=\infty} \\ &\quad = \frac{\lambda^2}{16\pi^4}\left(\frac{\cosh\theta-1}{2\sinh\theta}\right)^2 \int_a^{\infty}\frac{ds}{s}\ln\left(\frac{b+s\,e^{\theta}}{b+s\,e^{-\theta}}\right)\ln\left(\frac{s+b\,e^{\theta}}{s+b\,e^{-\theta}}\right) \end{aligned} \tag{5.10}$$

so that

$$\begin{aligned} &-\left(a\frac{d}{da}+b\frac{d}{db}\right)F_2(S,T;a,b)\Big|_{S=T=\infty} \\ &\quad = \frac{\lambda^2}{16\pi^4}\left(\frac{\cosh\theta-1}{2\sinh\theta}\right)^2 \int_0^{\infty}\frac{dz}{z}\ln\left(\frac{1+z\,e^{\theta}}{1+z\,e^{-\theta}}\right)\ln\left(\frac{z+e^{\theta}}{z+e^{-\theta}}\right). \end{aligned} \tag{5.11}$$

[5]Bateman manuscript on Higher Transcendental Functions, Sect. 1.11.1.

This expression is universal (does not depend on the ratio b/a) and reproduces the result (3.11) of Ref. [3] for the contribution of the ladders to the cusp anomalous dimension. We have therefore justified the procedure of Sect. 2 to use $a \sim \varepsilon$ and $b \sim \varepsilon$ as an ultraviolet cutoff.

5.2 Light-cone limit

As we have already pointed out, we are most interested in the limit of large θ when the cusp anomalous dimension reproduces the anomalous dimensions of twist-two conformal operators with large spin. As $\theta \to \infty$ one approaches the light-cone. Korchemsky and Marchesini [5] demonstrated how to calculate the cusp anomalous dimension directly from the light-cone Wilson loop:[6]

$$a\frac{\mathrm{d}}{\mathrm{d}a}\ln W\left(\Gamma_{\text{l.c.}}\right) = \frac{1}{4}f(\lambda)\ln\frac{T}{a}\,, \tag{5.12}$$

where $f(\lambda)$ is the same as in Eq. (1.1).

We can obtain the light-cone ladder equation either directly by summing the light-cone ladder diagrams or taking the $\theta \to \infty$ limit of the expressions in Eqs. (5.1) and (5.2). We find

$$G_\alpha\left(S,T;a,b\right) = 1 - \beta\int_a^S ds\int_b^T dt\,\frac{G_\alpha\left(S,T;s,t\right)}{\alpha s^2 + st}\,, \tag{5.13}$$

where

$$\beta = \frac{\lambda}{8\pi^2} \tag{5.14}$$

and we have redefined $T \to T/2$ and introduced

$$\alpha = \frac{u^2}{uv} = \pm 1 \tag{5.15}$$

(remember that $v^2 = 0$ for the light-cone direction). If we alternatively pick up the last (farthest from the cusp) rung of the ladder, we get

$$G_\alpha\left(S,T;a,b\right) = 1 - \beta\int_a^S ds\int_b^T dt\,\frac{G_\alpha\left(s,t;a,b\right)}{\alpha s^2 + st}\,. \tag{5.16}$$

These are of the type of Eqs. (5.1) and (5.2).

Differentiating Eq. (5.16) we obtain

$$S\frac{\partial}{\partial S}\,T\frac{\partial}{\partial T}\,G_\alpha\left(S,T;a,b\right) = -\frac{\beta}{1+\alpha S/T}\;G_\alpha\left(S,T;a,b\right). \tag{5.17}$$

The differentiation of Eq. (5.13) analogously gives

$$a\frac{\partial}{\partial a}\,b\frac{\partial}{\partial b}\,G_\alpha\left(S,T;a,b\right) = -\frac{\beta}{1+\alpha a/b}\;G_\alpha\left(S,T;a,b\right), \tag{5.18}$$

[6] An extra factor of $1/2$ in this formula is due to our regularization prescription.

while Eq. (5.4) is substituted by

$$F(S,T;a,b) = \beta \int_a^S ds \int_b^T dt \, \frac{1}{s(\alpha s + t)} + \int_a^S ds \int_b^T dt \, \frac{\partial F(s,t;a,b)}{\partial s} \frac{\partial F(s,t;a,b)}{\partial t} \, . \quad (5.19)$$

The differential equations (5.17) and (5.18) should be supplemented with the boundary conditions

$$G(a,T;a,b) = G(S,b;a,b) = 1 \, . \quad (5.20)$$

These boundary conditions follow from the integral equation (5.13) (or (5.16)).

Analogously to Eq. (5.5) we obtain

$$F_1(S,T;a,b) \;\; = \;\; \beta \left(L_2(-\frac{T}{\alpha S}) - L_2(-\frac{T}{\alpha a}) - L_2(-\frac{b}{\alpha S}) + L_2(-\frac{b}{\alpha a}) \right) . \quad (5.21)$$

Using Eq. (5.7), we can rewrite (5.21) in the equivalent form

$$F_1(S,T;a,b) = \beta \left(\ln \frac{T}{b} \ln \frac{S}{a} - L_2(-\alpha \frac{S}{T}) + L_2(-\alpha \frac{a}{T}) + L_2(-\alpha \frac{S}{b}) - L_2(-\alpha \frac{a}{b}) \right) . \quad (5.22)$$

This form is convenient to reproduce the order β of the $\alpha \to 0$ limit, when the exact G is given by the Bessel function

$$G_0 = J_0(2\sqrt{\beta \ln \frac{S}{a} \ln \frac{T}{b}}) \, . \quad (5.23)$$

The latter formula for the $\alpha = 0$ limit can be easily obtained by iterations of the ladder equation (5.13) (or (5.16)). Alternatively, the form (5.21) is convenient to find the $\alpha \to \infty$ limit.

We can also rewrite (5.21) as

$$F_1(S,T;a,b) = \beta \left(L_2(-\frac{T}{\alpha S}) + L_2(-\frac{\alpha a}{T}) + \frac{1}{2} \ln^2 \frac{T}{\alpha a} + \frac{\pi^2}{6} - L_2(-\frac{b}{\alpha S}) + L_2(-\frac{b}{\alpha a}) \right) . \quad (5.24)$$

If $S \to \infty$, we find from (5.24)

$$F_1(S=\infty,T;a,b) = \beta \left(\frac{1}{2} \ln^2 \frac{T}{\alpha a} + \frac{\pi^2}{6} + L_2(-\frac{b}{\alpha a}) + L_2(-\frac{\alpha a}{T}) \right) . \quad (5.25)$$

Remember that $L_2(0) = 0$ (associated with $b = 0$), $L_2(-1) = -\pi^2/12$ from Eq. (5.7) (associated with $\alpha a = b = \epsilon$) and $L_2(1) = \pi^2/6$ from Eq. (5.7) (associated with $\alpha = -1$, $a = b = \varepsilon$).

For $S \sim T \gg a, b$, we have from (5.24)

$$F_1(S,T;a,b) \stackrel{S,T \gg a,b}{=} \beta \left(L_2(-\frac{T}{\alpha S}) + \frac{1}{2} \ln^2 \frac{T}{\alpha a} + \frac{\pi^2}{6} + L_2(-\frac{b}{\alpha a}) \right) \quad (5.26)$$

and

$$F_1(S=\infty,T;a,b) \stackrel{T\gg a,b}{=} \beta\left(\frac{1}{2}\ln^2\frac{T}{\alpha a}+\frac{\pi^2}{6}+L_2(-\frac{b}{\alpha a})\right). \tag{5.27}$$

The order β^2 can be obtained by inserting (5.21) into the second term on the right-hand side of Eq. (5.4). This gives

$$F_2(S,T;a,b)=\beta^2\int_a^S ds_1\int_b^T dt_2\int_b^{t_2}\frac{dt_1}{s_1(\alpha s_1+t_1)}\int_a^{s_1}\frac{ds_2}{s_2(\alpha s_2+t_2)} \tag{5.28}$$

which is nothing but the light-cone diagram with crossed ladders. Integrating over s_2 and t_1, we find

$$F_2(S,T;a,b)=\beta^2\int_a^S\frac{ds}{s}\int_b^T\frac{dt}{t}\ln\frac{\alpha+t/s}{\alpha+b/s}\ln\frac{\alpha+t/a}{\alpha+t/s}. \tag{5.29}$$

Also we obtain

$$\left(a\frac{d}{da}\right)^2 F_2(S=\infty,T;a,b)$$
$$\stackrel{T\gg a,b}{=}\beta^2\left[\frac{1}{2}\ln^2\frac{T}{\alpha a}+\frac{\pi^2}{6}+L_2(-\frac{b}{\alpha a})-\ln\left(1+\frac{b}{\alpha a}\right)\ln\frac{(\alpha a+b)}{T}\right]. \tag{5.30}$$

With logarithmic accuracy this yields

$$F_2(S=\infty,T;a,b\sim a)\stackrel{T\gg a}{=}\beta^2\left(\frac{1}{24}\ln^4\frac{T}{\alpha a}+\frac{\pi^2}{12}\ln^2\frac{T}{\alpha a}\right). \tag{5.31}$$

The second term on the right-hand side of Eq. (5.31) is of the same type as in (5.25) which contributes to the cusp anomalous dimension. For $\alpha=1$ it agrees with Eq. (3.15).

For $\alpha=-1$ we get from Eq. (5.31)

$$\mathrm{Re}\,F_2(S=\infty,T;a,b\sim a)\stackrel{T\gg a}{=}\beta^2\left(\frac{1}{24}\ln^4\frac{T}{a}-\frac{\pi^2}{6}\ln^2\frac{T}{a}\right) \tag{5.32}$$

again with logarithmic accuracy. This is to be compared with the evaluation of the integral on the right-hand side of Eq. (5.29) for $S=T$, $b=a$ and $\alpha=-1$ which results in the exact formula

$$\mathrm{Re}\,F_2(S=T;a=b)\stackrel{\alpha=-1}{=}\beta^2\left(\frac{1}{24}\ln^4\frac{T}{a}-\frac{\pi^2}{6}\ln^2\frac{T}{a}\right) \tag{5.33}$$

for all values of T. The fact that the $\ln^2(T/a)$ term is the same as in Eq. (5.32) confirms the expectation that the cusp anomalous dimension can be extracted from the $S\sim T\gg a\sim b$ limit, which is based on the fact that Log's of S/a never appear in perturbation theory.

The appearance of the $\ln^4(T/a)$ term in Eqs. (5.31) and (5.32) implies no exponentiation for the ladder diagrams. It is already known from Sect. 3 that the exponentiation occurs only when the ladders are summed up with the anomalous term observed in Sect. 2.

5.3 Exact solution for light-cone ladders

To satisfy Eqs. (5.17) and (5.18), we substitute the ansatz

$$G_\alpha\left(S,T;a,b\right)=\oint\limits_C\frac{d\omega}{2\pi i\omega}\left(\frac{S}{a}\right)^{\sqrt{\beta}\omega}\left(\frac{T}{b}\right)^{-\sqrt{\beta}\omega^{-1}}F\left(-\omega,\alpha\frac{a}{b}\right)F\left(\omega,\alpha\frac{S}{T}\right), \tag{5.34}$$

where C is a contour in the complex ω-plane. This ansatz is motivated by the integral representation of the Bessel function (5.23) at $\alpha=0$. The substitution into Eq. (5.17) reduces it to the hypergeometric equation ($\xi=\alpha S/T$)

$$\xi(1+\xi)F''_{\xi\xi}+[1+\sqrt{\beta}(\omega+\omega^{-1})](1+\xi)F'_\xi+\beta F=0 \tag{5.35}$$

whose solution is given by hypergeometric functions. The same is true for Eq. (5.18) when ω is substituted by $-\omega$ and $\xi=\alpha a/b$.

We have shown that the following combination of solutions satisfies the boundary conditions (5.20):

$$\begin{aligned}
G_\alpha(S,T;a,b)=&\oint\limits_{C^r}\frac{d\omega}{2\pi i\omega}\,{}_2F_1\left(-\sqrt{\beta}\omega,-\sqrt{\beta}\omega^{-1};1-\sqrt{\beta}(\omega+\omega^{-1});-\alpha\frac{a}{b}\right)\\
&\times\left(\frac{S}{a}\right)^{\sqrt{\beta}\omega}\left(\frac{T}{b}\right)^{-\sqrt{\beta}\omega^{-1}}{}_2F_1\left(\sqrt{\beta}\omega,\sqrt{\beta}\omega^{-1};1+\sqrt{\beta}(\omega+\omega^{-1});-\alpha\frac{S}{T}\right)\\
+&\int_{|_{n_{\min}-0}}\frac{ds}{2\pi i}\frac{\Gamma(-s)}{\Gamma(s)}\frac{1}{\sqrt{\beta}(\omega_+^R-\omega_-^R)}\frac{\Gamma(\sqrt{\beta}\omega_+^R)\Gamma(1+\sqrt{\beta}\omega_+^R)}{\Gamma(\sqrt{\beta}\omega_+^L)\Gamma(1+\sqrt{\beta}\omega_+^L)}\\
&\times\left(\alpha\frac{a}{b}\right)^s\left[\left(\frac{S}{a}\right)^{\sqrt{\beta}\omega_+^R}\left(\frac{T}{b}\right)^{-\sqrt{\beta}\omega_-^R}+\left(\frac{S}{a}\right)^{\sqrt{\beta}\omega_-^R}\left(\frac{T}{b}\right)^{-\sqrt{\beta}\omega_+^R}\right]\\
&\times{}_2F_1\left(\sqrt{\beta}\omega_+^R,\sqrt{\beta}\omega_-^R;s+1;-\alpha\frac{a}{b}\right){}_2F_1\left(\sqrt{\beta}\omega_+^R,\sqrt{\beta}\omega_-^R;s+1;-\alpha\frac{S}{T}\right)
\end{aligned} \tag{5.36}$$

with

$$\begin{aligned}
\omega_\pm^R(s)&=\frac{s}{2\sqrt{\beta}}\pm\sqrt{\frac{s^2}{4\beta}-1}\,,\\
\omega_\pm^L(s)&=-\omega_\mp^R=-\frac{s}{2\sqrt{\beta}}\pm\sqrt{\frac{s^2}{4\beta}-1}\,.
\end{aligned} \tag{5.37}$$

The contour integral in the first term on the right-hand side of Eq. (5.36) runs over a circle of arbitrary radius r ($|\omega|=r$), while the second contour integral runs parallel to imaginary axis along the line

$$s=n_{\min}-0+ip\qquad(-\infty<p<+\infty)\,, \tag{5.38}$$

where

$$n_{\min} = \left[\sqrt{\beta}(r + 1/r)\right] + 1 \tag{5.39}$$

and $[\cdots]$ denotes the integer part.

Each of the two terms on the right-hand side of Eq. (5.36) satisfies the linear differential equations (5.17) and (5.18). They are added in the way to satisfy the boundary conditions (5.20).

To show this, it is crucial that the poles at $\omega = \omega_{\pm}^{R}(n)$ and $\omega = \omega_{\pm}^{L}(n)$ of the integrand in the first term are canceled by the poles at $s = n$ of the integrand in the second term. The position of the real part of the contour of integration over s is such to match the number of poles. If $r < 1$ the poles at $\omega_{-}^{R}(n)$ and $\omega_{+}^{L}(n)$ lie inside the circle of integration for $\sqrt{\beta} < (r + r^{-1})^{-1}$. This corresponds to $n_{\min} = 1$ in Eq. (5.39) so that all poles of the integrand in the second term are to the right of the integration contour over s. The residues are chosen to be the same. At $\sqrt{\beta} = (r + r^{-1})^{-1}$ the poles at $\omega_{-}^{R}(1)$ and $\omega_{+}^{L}(1)$ crosses the circle of integration and correspondingly the contour of integration over s jumps toward $\mathrm{Re}\, s = 2$ because now $n_{\min} = 2$. With increasing $\sqrt{\beta}$ the poles at $\omega_{-}^{R}(n)$ and $\omega_{+}^{L}(n)$ with $n \geq n_{\min}$ of the integrand in the first term, which lie inside the circle of integration, are canceled by the poles at $s = n \geq n_{\min}$ of the integrand in the second term. A useful formula which provides the cancellation is

$${}_2F_1(A, B; C; z) \overset{C \to -n+1}{\longrightarrow} \Gamma(C) \frac{\Gamma(A+n)\Gamma(B+n)}{\Gamma(A)\Gamma(B)\, n!}\, z^n {}_2F_1(A+n, B+n; n+1; z) \tag{5.40}$$

as $C \to -n + 1$.

To demonstrate how the boundary conditions (5.20) are satisfied by the solution (5.36), we choose the integration contour in the first term to be a circle of the radius which is either very small for $T = b$ or very large for $S = a$. Then the form of the integrand is such that the residue at the pole, respectively, at $\omega = 0$ or $\omega = \infty$ equals 1 which proves that the boundary conditions is satisfied.

The numerical value of G given by Eq. (5.36) can be computed for a certain range of the parameters S, T, b and α using the Mathematica program in Appendix A.

5.4 Exact solution for light-cone ladders (continued)

A great simplification occurs in Eq. (5.36) for $\alpha = -1$, $S = T$ and $b = a$, when the hypergeometric functions reduce to gamma functions:

$${}_2F_1\left(A, B; 1 + A + B; 1\right) = \frac{\Gamma\left(1 + A + B\right)}{\Gamma\left(1 + A\right)\Gamma\left(1 + B\right)}\,. \tag{5.41}$$

We then obtain

$$G_{\alpha=-1}(T,T;a,a) = \oint\limits_{C^r} \frac{d\omega}{2i\pi^2\sqrt{\beta}\omega} \left(\frac{T}{a}\right)^{\sqrt{\beta}(\omega-\omega^{-1})} \frac{\sin(\pi\sqrt{\beta}\omega)\sin(\pi\sqrt{\beta}\omega^{-1})}{\sin(\pi\sqrt{\beta}(\omega+\omega^{-1}))}(\omega+\omega^{-1}) + \int_{|_{n_{\min}-0}} \frac{ds}{2i\beta\pi^2}\frac{s(-1)^s}{\sin(\pi s)}\frac{\sin^2(\pi\sqrt{\beta}\omega_-^R)}{\sqrt{\beta}(\omega_+^R-\omega_-^R)}\left[\left(\frac{T}{a}\right)^{\sqrt{\beta}(\omega_+^R-\omega_-^R)} + \left(\frac{T}{a}\right)^{\sqrt{\beta}(\omega_-^R-\omega_+^R)}\right]. \tag{5.42}$$

We can now make a change of the integration variable in the first contour integral from ω to

$$s = \sqrt{\beta}(\omega+\omega^{-1}) \tag{5.43}$$

so that

$$\frac{d\omega}{\omega} = \frac{ds}{\sqrt{s^2-4\beta}} \tag{5.44}$$

and rewrite Eq. (5.42) as

$$\begin{aligned} &G_{\alpha=-1}(T,T;a,a) \\ &= \int\limits_{-2\sqrt{\beta}}^{+2\sqrt{\beta}} \frac{ds}{2\pi^2\beta}\frac{s}{\sqrt{\beta-s^2/4}}\left(\frac{T}{a}\right)^{\sqrt{\beta}(\omega_+^R-\omega_-^R)} \frac{\sin(\pi\sqrt{\beta}\omega_+^R)\sin(\pi\sqrt{\beta}\omega_-^R)}{\sin(\pi s)} \\ &\quad + \int_{|_{n_{\min}-0}} \frac{ds}{2i\beta\pi^2}\frac{s(-1)^s}{\sin(\pi s)}\frac{\sin^2(\pi\sqrt{\beta}\omega_-^R)}{\sqrt{\beta}(\omega_+^R-\omega_-^R)}\left[\left(\frac{T}{a}\right)^{\sqrt{\beta}(\omega_+^R-\omega_-^R)} + \left(\frac{T}{a}\right)^{\sqrt{\beta}(\omega_-^R-\omega_+^R)}\right]. \end{aligned} \tag{5.45}$$

The integrand of the first term on the right-hand side may have poles for $\beta > 1/4$ at $s = \pm n$. Then it should be understood as the principal value integral.

For $\sqrt{\beta} < 1/2$ we can first substitute $s \to -s$ in the second term in the square brackets in the last line of Eq. (5.45) to get the integral over $\mathrm{Re}\, s = -1$ and then to deform the contour of the integration from $\mathrm{Re}\, s = \pm 1$ to obtain the same contour as in the first integral on the right-hand side.

We then rewrite Eq. (5.45) as

$$\begin{aligned} &G_{\alpha=-1}(T,T;a,a) \\ &= \int\limits_{-2\sqrt{\beta}}^{+2\sqrt{\beta}} \frac{ds}{2\pi^2\beta}\frac{s\sin(\pi s)}{\sqrt{4\beta-s^2}}\cos\left(\sqrt{4\beta-s^2}(\ln\frac{T}{a}-i\pi)\right)\sin\left(\pi\sqrt{4\beta-s^2}\right). \end{aligned} \tag{5.46}$$

Consulting with the table of integrals[7], we finally express the integral in Eq. (5.46) via the Bessel function

$$G_{\alpha=-1}(ae^{\tau},ae^{\tau};a,a) = \frac{1}{\sqrt{\beta\tau(\tau-2\pi i)}}J_1\left(2\sqrt{\beta\tau(\tau-2\pi i)}\right) \tag{5.47}$$

[7]I.S. Gradshteyn and I.M. Ryzhik, Table of integrals, series and products, Eq. 3.876.7 on p. 473.

with

$$\ln\frac{T}{a}=\tau,\qquad \ln\left(-\frac{T}{a}\right)=\tau-i\pi \tag{5.48}$$

and β given by Eq. (5.14). Note this is J_1 rather than I_1 as in Ref. [21] because of Minkowski space.

Taking according to Eq. (5.3) $-$Log of the expansion of (5.47) in β, we get

$$\begin{aligned} F_{\alpha=-1}(ae^{\tau},ae^{\tau};a,a) &= \frac{1}{2}\Big(\beta\tau(\tau-2\pi i)\Big)+\frac{1}{24}\Big(\beta\tau(\tau-2\pi i)\Big)^2+\frac{1}{144}\Big(\beta\tau(\tau-2\pi i)\Big)^3 \\ &\quad +\frac{1}{720}\Big(\beta\tau(\tau-2\pi i)\Big)^4+\mathcal{O}\left(\beta^5\right). \end{aligned} \tag{5.49}$$

The order β^2 is in a perfect agreement with Eq. (5.32). We see that only the first two ladders have a τ^2 term and, therefore, contribute to the cusp anomalous dimension.

5.5 Asymptotic behavior

It is easy to write down the asymptote of the solution (5.47) at large $\tau=\ln\frac{T}{a}$:

$$G_{\alpha=-1}(ae^{\tau},ae^{\tau};a,a)\overset{\tau\gg1}{\approx}\cos\left(2\sqrt{\beta}\tau-\frac{3\pi}{4}\right)\frac{1}{\sqrt{\pi}(\sqrt{\beta}\tau)^{3/2}}\,. \tag{5.50}$$

One may wonder how this asymptote can be extended to the case of $S\neq T$, in particular $S\gg T$.

Rewriting the differential ladder equation (5.17) via the variables

$$x=\ln\frac{S}{a}-\ln\frac{T}{a}\,,\qquad y=\ln\frac{S}{a}+\ln\frac{T}{a}\,, \tag{5.51}$$

we obtain

$$\left(\frac{\partial^2}{\partial x^2}-\frac{\partial^2}{\partial y^2}\right)G(x,y)=\frac{\beta}{1-e^x}\,G(x,y) \tag{5.52}$$

for $\alpha=-1$ and $b=a$.

The existence of the stationary-phase points of both integrals on the right-hand side of Eq. (5.45) at $s=0$ valid for $S=T$ suggests to satisfy Eq. (5.52) at large β by introducing a phase in the argument of the cosine in Eq. (5.50):

$$\cos\left(2\sqrt{\beta}\tau-\frac{3\pi}{4}\right)\Longrightarrow\cos\left(\sqrt{\beta}y-\sqrt{\beta}\varphi(x)-\frac{3\pi}{4}\right). \tag{5.53}$$

Then Eq. (5.52) is satisfied by the cosine for large β if

$$\varphi(x)=2\,\mathrm{arccosh}\,e^{x/2} \tag{5.54}$$

which obeys $\varphi(0)=0$ as it should. In a more rigorous treatment the cosine should of course be multiplied by a decreasing prefactor.

As we expected from the analysis of perturbation theory, where each term remains finite as $S \to \infty$, the arguments of the cosine on both sides of Eq. (5.53) should remain the same with logarithmic accuracy as $S \to \infty$. This is indeed the case for the solution (5.54) which behaves at large x as

$$\varphi(x) = x - 2\ln 2 + \mathcal{O}(x^{-1})\,, \tag{5.55}$$

so that we find

$$\cos\left(\sqrt{\beta}y - \sqrt{\beta}\varphi(x) - \frac{3\pi}{4}\right) \overset{S\to\infty}{=} \cos\left(2\sqrt{\beta}\tau + 2\sqrt{\beta}\ln 2 - \frac{3\pi}{4}\right). \tag{5.56}$$

This type of the asymptotic behavior is not of the type given by Eq. (5.12) and leads us to the conclusion that the ladder diagrams cannot reproduce the $\sqrt{\lambda}$-behavior of the cusp anomalous dimension for large λ.

6 Discussion

The main conclusion of this paper is that the cusped Wilson loop possesses a number of remarkable dynamical properties which make it a very interesting object for studying the string/gauge correspondence. On one hand its dynamics in $\mathcal{N} = 4$ SYM is more complicated than that of the solvable cases of the straight line or circular loop and it therefore is a more powerful probe of the gauge theory. On the other hand it has certain simple features which could be accessible to analytic computations and which could be universal, in the sense that they are shared by non-supersymmetric Yang-Mills theory or even QCD.

An example of the latter is the appearance of the anomaly term in the two-loop calculations of this paper. Unlike the case of smooth loops, the cancellation of the divergent parts of Feynman diagrams with internal vertices is not complete. What remains has a nice simple structure of an "anomalous surface term" where some legs of the diagrams with internal vertices are frozen onto the cusp. This is reminiscent of the anomaly explanation of the simple structure of the circular loop and its subsequent relation to a one-matrix model presented in Ref. [23]. In the case of the cusp, the "degrees of freedom" which give rise to the divergent part of the expectation value seem to reside at the location of the cusp. We expect this to persist in higher orders of perturbation theory. The fact that the sum of all ladders does not seem to contribute to the leading term in the cusp anomalous dimension means that the entire contribution, if it is indeed there, comes from diagrams with internal vertices. We expect that such diagrams all have legs frozen at the location of the cusp like the diagram depicted in Fig. 3(a). It would be interesting to try to characterize these diagrams and understand the generic contribution.

Analogously, the loop equation reveals a number of interesting properties which are specific to the cusped loop. Here, we have checked that the appearance of the cusp anomalous dimension in the supersymmetric loop equation observed to one-loop in Ref. [17],

actually persists at two loop order. This involves some non-trivial and rather surprising identities for integrals that we have detailed in Sect. 4.

Finally, the sum of the ladder diagrams can be found exactly and for certain values of parameters reduces to the Bessel function. In fact, the Bessel function is very similar to the one that is thought to be the exact expression for the circular loop [21].

It is not yet clear which of these features are common with usual Yang-Mills theory, but some of them certainly are. One of such quantity is the universal part of the cusp anomalous dimension in pure QCD at two loops, which does not depend on the regularization prescription. It may support the expectation put forward in Ref. [7] that the universal part of the anomalous dimensions of twist-two operators with large spin J in pure Yang-Mills theory and $\mathcal{N}=4$ SYM are in fact identical.

In order to clarify this assertion, we compare the anomalous dimension of the cusped SYM Wilson loop, calculated in this paper, with the analogous calculation of the one for the properly regularized non-supersymmetric Wilson loop of only Yang-Mills field in Yang-Mills theory with adjoint matter. While the fermionic contribution has been known for a while [3], the contribution from scalars has been calculated relatively recently [32]. The result is given at large θ by

$$\gamma_{\rm cusp}=\frac{\theta}{2}\left[\frac{\lambda}{2\pi^2}+\frac{\lambda^2}{24\pi^4}\left(\frac{16}{3}-\frac{\pi^2}{4}-\frac{5}{6}n_f-\frac{1}{3}n_s\right)\right]+\mathcal{O}\left(\lambda^3\right), \tag{6.1}$$

where n_f is the number fermionic species and n_s is the number of scalars (which are present only in the action but not in the definition of the Wilson loop as is already said). The pure Yang-Mills contribution (associated with $n_f=n_s=0$) is regularization-dependent at order λ^2 and has a universal part $\propto\lambda^2/\pi^2$ as well as the regularization-dependent part $\propto\lambda^2/\pi^4$. Here, the latter, regularization-dependent part is written for regularization via dimensional reduction (the DR scheme).

For the $\mathcal{N}=4$ SYM we substitute in Eq. (6.1) $n_f=4$ and $n_s=6$ after which the non-universal part vanishes and we reproduce Eq. (3.16). This means that the only effect of scalars (as well as of fermions) is their contribution to the renormalization of the coupling constant, while they decouple from the supersymmetric light-cone Wilson loop because $\dot{x}^2=0$ at the light-cone.

For the latter reason it would be interesting to investigate loop equation (4.1) for supersymmetric cusped Wilson loops in $\mathcal{N}=4$ SYM. A nice property of this equation is that the contribution of scalars to the right-hand side vanishes at the light-cone. The cusped loop equation, which sums up all relevant planar diagrams, can be also useful for calculations of the cusp anomalous dimension. In fact the structure of the right-hand side of Eq. (4.1) is such that it involves only one cusped Wilson loop while another W is rather a Bethe-Salpeter kernel of the type calculated in this paper. These issues deserve further investigation.

Acknowledgments

Y.M. is indebted to J. Ambjørn, A. Gorsky, H. Kawai, L. Lipatov, J. Maldacena, A. Tseytlin, and K. Zarembo for useful discussions. The work of Y.M. was partially supported by the Federal Program of the Russian Ministry for Industry, Science and Technology No 40.052.1.1.1112. The work of Y.M. and P.O. was supported in part by the grant INTAS 03–51–5460. The work of Y.M. and G.S. was supported in part by the grant NATO CLG–5941. G.S. acknowledges financial support of NSERC of Canada.

Appendix A Program for computing (5.36)

```
(* the value of x = Sqrt[beta] *)
x =.
(* the values of S, T, b, al = alpha *)
S = 100
T = 100
a = 1
b = a
al = 1
R = .8
(* residues are summed up from n = Real[s] + 1 *)
s[x_, p_] := IntegerPart[x(R + 1/R)] + .9999 + I p
ORp[ss_] := ss/2 + Sqrt[ss^2/4 - x^2]
ORm[ss_] := ss/2 - Sqrt[ss^2/4 - x^2]
OLp[ss_] := -ss/2 + Sqrt[ss^2/4 - x^2]
OLm[ss_] := -ss/2 - Sqrt[ss^2/4 - x^2]
(* enumeration of the contour integral *)
Int[x_, T_] := NIntegrate[ (S/a)^(x R Exp[I phi])
   (T/b)^(-x R^(-1)Exp[-I phi])
   Hypergeometric2F1[-x R Exp[I phi], -x R^(-1)Exp[-I phi],
      1 - x R Exp[I phi] - x R^(-1)Exp[-I phi], -al a/b]
   Hypergeometric2F1[x R Exp[I phi], x R^(-1)Exp[-I phi],
      1 + x R Exp[I phi] + x R^(-1)Exp[-I phi], -al S/T]/(2 Pi),
    {phi, 0, 2 Pi}, MaxRecursion -> 16]
(* the sum over residues inside the circle *)
Res[x_, T_] :=
  NIntegrate[(Gamma[-s[x, p]]/
          Gamma[s[x, p]])(ORp[s[x, p]] - ORm[s[x, p]])^(-1)( al a/b)^
        s[x, p](Gamma[ORp[s[x, p]]]Gamma[ORp[s[x, p]] +
                1]/(Gamma[OLp[s[x, p]]]Gamma[OLp[s[x, p]] + 1]))
                  ((S/a)^(ORp[s[x, p]])(T/b)^(-ORm[s[x, p]])
```

```
                    + (S/a)^(ORm[s[x, p]])(T/b)^(-ORp[s[x, p]]))
   Hypergeometric2F1[-OLp[s[x, p]], -OLm[s[x, p]], 1 + s[x, p], -al a/b]
   Hypergeometric2F1[ORp[s[x, p]], ORm[s[x, p]],
          1 + s[x, p], -al S/T]/(2 Pi), {p, -Infinity, +Infinity},
    MaxRecursion -> 16]
G[x_, T_] := Int[x, T] + Res[x, T]
    (* G[x, T] *)
Plot[G[x, T], {x, 0, 3.}]
```

References

[1] Y. Makeenko, *Methods of contemporary gauge theory*, Cambridge Univ. Press 2002, pp. 252–254.

[2] N. S. Craigie and H. Dorn, *On the renormalization and short distance properties of hadronic operators in QCD*, Nucl. Phys. B **185** (1981) 204.

[3] G. P. Korchemsky and A. V. Radyushkin, *Renormalization of the Wilson loops beyond the leading order*, Nucl. Phys. B **283** (1987) 342.

[4] I. I. Balitsky and V. M. Braun, *Evolution equations for QCD string operators*, Nucl. Phys. B **311** (1988) 541.

[5] G. P. Korchemsky and G. Marchesini, *Partonic distributions for large x and renormalization of Wilson loop*, Nucl. Phys. B **406** (1993) 225.

[6] S. J. Brodsky, Y. Frishman, G. P. Lepage and C. T. Sachrajda, *Hadronic wave functions at short distances and the operator product expansion,* Phys. Lett. B **91** (1980) 239;
Y. M. Makeenko, *On conformal operators in quantum chromodynamics,* Sov. J. Nucl. Phys. **33** (1981) 440;
T. Ohrndorf, *Constraints from conformal covariance on the mixing of operators of lowest twist,* Nucl. Phys. B **198** (1982) 26.

[7] S. S. Gubser, I. R. Klebanov and A. M. Polyakov, *A semi-classical limit of the gauge/string correspondence*, Nucl. Phys. B **636** (2002) 99 [hep-th/020405].

[8] J. Maldacena, *The large N limit of super-conformal field theories and supergravity,* Adv. Theor. Math. Phys. **2** (1998) 231 [hep-th/9711200].

[9] S. S. Gubser, I. R. Klebanov and A. M. Polyakov, *Gauge theory correlators from non-critical string theory,* Phys. Lett. B **428** (1998) 105 [hep-th/9802109].

[10] E. Witten, *Anti-de Sitter space and holography,* Adv. Theor. Math. Phys. **2** (1998) 253 [hep-th/9802150].

[11] O. Aharony, S. S. Gubser, J. Maldacena, H. Ooguri and Y. Oz, *Large N field theories, string theory and gravity,* Phys. Rep. **323** (2000) 183 [hep-th/9905111].

[12] S. Frolov, A. A. Tseytlin *Semiclassical quantization of rotating superstring in $AdS_5 \times S^5$,* JHEP **0206** (2002) 007 [hep-th/0204226].

[13] D. Berenstein, J. Maldacena and H. Nastase, *Strings in flat space and pp waves from $\mathcal{N} = 4$ super Yang Mills*, JHEP **0204** (2002) 013 [hep-th/0202021].

[14] J. Maldacena, *Wilson loops in large N field theories*, Phys. Rev. Lett. **80** (1998) 4859 [hep-th/9803002].

[15] S.-J. Rey and J. Yee, *Macroscopic strings as heavy quarks in large N gauge theory and anti-de Sitter supergravity,* Eur. Phys. J. C **22** (2001) 379 [hep-th/9803001].

[16] D. Berenstein, R. Corrado, W. Fischler and J. Maldacena, *The operator product expansion for Wilson loops and surfaces in the large N limit,* Phys. Rev. D **59** (1999) 105023 [hep-th/9809188].

[17] N. Drukker, D. J. Gross and H. Ooguri, *Wilson loops and minimal surfaces*, Phys. Rev. D **60** (1999) 125006 [hep-th/9904191].

[18] M. Kruczenski, *A note on twist two operators in $\mathcal{N} = 4$ SYM and Wilson loops in Minkowski signature*, JHEP **0212** (2002) 024 [hep-th/0210115].

[19] Y. Makeenko, *Light-cone Wilson loops and the string/gauge correspondence,* JHEP **0301** (2003) 007 [hep-th/0210256].

[20] J. K. Erickson, G. W. Semenoff, R. J. Szabo, and K. Zarembo, *Static potential in $\mathcal{N} = 4$ supersymmetric Yang-Mills theory,* Phys. Rev. D **61** (2000) 105006 [hep-th/9911088].

[21] J. K. Erickson, G. W. Semenoff and K. Zarembo, *Wilson loops in $\mathcal{N} = 4$ supersymmetric Yang-Mills theory,* Nucl. Phys. B **582** (2000) 155 [hep-th/0003055].

[22] G. W. Semenoff and K. Zarembo, *More exact predictions of SUSYM for string theory,* Nucl. Phys. B **616** (2001) 34 [hep-th/0106015].

[23] N. Drukker and D. J. Gross, *An exact prediction of $\mathcal{N} = 4$ SUSYM theory for string theory,* J. Math. Phys. **42** (2001) 2896 [hep-th/0010274].

[24] G. W. Semenoff and K. Zarembo, *Wilson loops in SYM theory: from weak to strong coupling,* Nucl. Phys. Proc. Suppl. **108** (2002) 106 [hep-th/0202156].

[25] A. Gonzalez-Arroyo and C. Lopez, *Second-order contribution to the structure functions in deep inelastic scattering (III)*, Nucl. Phys. B **166** (1980) 429.

[26] A. V. Kotikov and L. N. Lipatov, *NLO corrections to the BFKL equation in QCD and in supersymmetric gauge theories,* Nucl. Phys. B **582** (2000) 19 [hep-ph/0004008].

[27] A. V. Kotikov and L. N. Lipatov, *DGLAP and BFKL equations in the $\mathcal{N} = 4$ supersymmetric gauge theory*, Nucl. Phys. B **661** (2003) 19 [hep-ph/0208220].

[28] M. Axenides, E. Floratos and A. Kehagias, *Scaling violations in Yang-Mills theories and strings in AdS_5,* Nucl. Phys. B **662** (2003) 170 [hep-th/0210091].

[29] A. V. Kotikov, L. N. Lipatov and V. N. Velizhanin, *Anomalous dimensions of Wilson operators in $\mathcal{N} = 4$ SYM theory,* Phys. Lett. B **557** (2003) 114 [hep-ph/0301021].

[30] A. V. Kotikov, L. N. Lipatov, A. I. Onishchenko, and V. N. Velizhanin, *Three-loop universal anomalous dimension of the Wilson operators in $\mathcal{N} = 4$ SUSY Yang-Mills model,* Phys. Lett. B**595** (2004) 521 [hep-th/0404092].

[31] M. Staudacher, *The factorized S-matrix of CFT/AdS*, JHEP **0505** (2005) 054 [hep-th/0412188].

[32] A. V. Belitsky, A. S. Gorsky and G. P. Korchemsky, *Gauge/string duality for QCD conformal operators,* Nucl. Phys. B **667** (2003) 3 [hep-th/0304028].

[33] G. W. Semenoff and D. Young, *Wavy Wilson line and AdS/CFT,* Int. J. Mod. Phys. A **20** (2005) 2833 [hep-th/0405288].

[34] Y. M. Makeenko and A. A. Migdal, *Exact equation for the loop average in multicolor QCD,* Phys. Lett. B **88** (1979) 135.

[35] Y. M. Makeenko, *Polygon discretization of the loop space equation,* Phys. Lett. B **212** (1988) 221.

[36] M. Fukuma, H. Kawai, Y. Kitazawa and A. Tsuchiya, *String field theory from IIB matrix model,* Nucl. Phys. B **510** (1998) 158 [hep-th/9705128].

[37] Y. Makeenko and A. A. Migdal, *Quantum chromodynamics as dynamics of loops,* Nucl. Phys. B **188** (1981) 269.